Caspian Journal of Environmental Sciences
Online ISSN: 1735-3866
Print ISSN: 1735-3033

How do blue ecosystem services respond to drought resulting from climate change?

Mohammad Ali Gholami Sefidkouhi[1], Sareh Hosseini[2]*, Fahimeh Karimpour[1], Hanieh Masri[1], Erfan Hosseini[1]

1. Department of Water Engineering, Sari Agricultural Sciences and Natural Resources University, Sari, Iran
2. Department of Forest Science and Engineering, Faculty of Natural Resources, University of Guilan, Sowmeh Sara, Guilan, Iran

* *Corresponding author's E-mail: S.hosseini@Guilan.ac.ir*

ABSTRACT

Climate changes have a significant impact on the blue ecosystem especially watershed's ecosystem services. Nowadays, increasing air Temperature (Ta), Land Surface Temperature (LST) and drought are consequences of climate change affecting the access to water sources directly. The aim of this study is to evaluate the climate change effects on the ecosystem services such as Ta and LST regulation and drought reduction in the Tajan watershed, Northern Iran. Landsat 8 OLI satellite images used to investigate LST and drought indices include Vegetation Health Index (VHI), Temperature Condition Index (TCI), Vegetation Condition Index (VCI), Soil Adjusted Vegetation Index (SAVI) and Normalized Difference Vegetation Index (NDVI) from July to September during 2013 to 2023. The results indicated that the LST minimum and maximum value at Tajan watershed had an upward trend from 2013 to 2022. In other words, the mean value of LST increased by 8 ℃ in the watershed during the period of 10 years. Also, analyzing drought indices showed that the drought has increased significantly in the central, eastern, and southeastern parts of Tajan watershed from 2013 to 2022. The drought indices results demonstrated that vegetation cover and climate change have significant effects on LST trends. Therefore, it can be said that climate change, vegetation cover destruction and also converting forests and agriculture land to residential and barren lands increase the LST and drought in Tajan watershed, hence significantly impact on its ecosystem services. Findings indicated that severe drought and heat islands will occur in Tajan watershed in the future.

Keywords: Vegetation, Drought, Land use, Thermal islands, Tajan watershed.
Article type: Research Article.

INTRODUCTION

Blue ecosystems are considered one of the most obvious natural ecosystems that provide valuable services such as water regulation and supply, flood reduction, microclimate regulation, air Temperature (Ta), Land Surface Temperature (LST) regulation, drought reduction, aquatic habitat and other services for ecosystem residents and beneficiaries (Ma *et al*. 2021; Hosseini *et al*. 2021; Uniyal *et al*. 2023; Amirnejad *et al*. 2025). Nowadays, population growth, cities development, environmental pollution, climatic change, land use change, and vegetation cover reduction have caused an increase in TA, LST, drought and water resources reduction (Zarandian *et al.* 2016; Jahanifar *et al.* 2017; Kapuka *et al*. 2022). So, the lack of water resources, climate change and the increase in LST caused by inappropriate human activities are of international community concern (Ketelsen *et al*. 2020; Ashrafi *et al*. 2022). Previous studies of the Intergovernmental Panel on Climate Change (IPCC) indicated that the global temperature average will elevate 2.4 ℃ by the end of this century, and these changes will be very large on a zonal scale (Harishnaika *et al*. 2022). Therefore, it has been more than a decade that LST has been studied to

understand climate change at the global level. The LST index is used to investigate the physical attributes of surface activities and climate changes (Kumari *et al*. 2021). Also, the LST has an important effect on the analysis of ecological issues as soil moisture, and vegetation cover urban heat islands (Zaharaddeen *et al*. 2016). However, due to the fact that the measurement of the LST is point-based and in principle, it cannot be obtained using measurements on the ground in large areas. Satellite images are a suitable tool for the LST extracting and measuring (Feng *et al*. 2019). Between the remote sensing (RS) thermal data, satellite images such as MODIS, Aster, and Landsat have a special role in estimating LST due to having thermal bands (Mulugeta *et al*. 2019; Guha *et al*. 2020). In particular, the Landsat 8 satellite thermal sensors provide a better representation of the LST and it can be a suitable reference for measuring the temperature and checking the LST in future studies (Chang *et al*. 2021). Natural and human activities affect the LST and cause vegetation cover losing, local climate change and drought phenomenon. Drought is an unfortunate climatic phenomenon that directly affects communities through the restriction of access to water resources and brings many economic, social and environmental costs (Xie &Fan 2021). Therefore, drought monitoring is very important. Drought can be evaluated using drought indices (Guo *et al*. 2017). So far, a lot of drought indices were introduced. The common point of all drought studies is that they use drought indices that weather elements are effective factors in their formation (Xie &Fan 2021). In the past, drought assessment was based on meteorological observations، statistics, and data from meteorological station, but the results were not sufficiently accurate due to the dispersion of meteorological stations from the study area (Wang *et al*. 2018). In the last four decades, RS using satellite images with high temporal and spatial resolution, wide coverage of the studied areas and direct investigation of vegetation status has played an important role in drought monitoring. Also, satellite indices have provided the title of drought monitoring tool (Elhag & Zhang 2018; Lei *et al*. 2019). Nowadays, many drought monitoring models performed according to LST, vegetation index, humidity, and reflectance at the visible and infrared regions (Bayarjargal *et al*. 2006). The indices including Vegetation Health Index (VHI), Vegetation Condition Index (VCI), Temperature Condition Index (TCI) (Kogan 1995), Soil Adjusted Vegetation Index (SAVI; Zhen *et al*. 2021) and Normalized Difference Vegetation Index (NDVI; Bai *et al*. 2012; Eze *et al*. 2020). Globally, drought monitoring has been widely done through various satellites such as AVHRR (Kong *et al*. 2019; Xie & Fan 2021), and MODIS (Rhee *et al*. 2010). However, few studies have been conducted about monitoring and investigating the climate change effect on the LST and its correlation with vegetation changes and drought indices using Landsat satellite images. Rongali *et al*. (2017) investigated the LST using Landsat 8 thermal bands and the single-window algorithm in the Beas river basin of India. The findings indicated that there is a strong relationship between vegetation and land surface temperature (LST). In addition, Wang *et al*. (2018) reported the capability of MODIS image data in investigating spatial-temporal changes of meteorological droughts in the Yellow River basin indicating a significant relationship among the results of the study and the indices of VCI, MTVDI, VHI, TCI, NDVI, and NVSWI in the years from 2001 to 2020. Also, Wang *et al*. (2019) studied Land Use Changes (LUC) and LST in the Pearl River delta of China in a time series. The finding indicated that the LST has increased due to the growth of urban areas and LUC. Sekertekin & Bonafoni (2020) investigated the LST using radiation transfer, single-window and single-channel algorithms. Three algorithms showed results specifically for calculating the land surface. Kloos *et al*. (2021) investigated agricultural drought using vegetation health indices and MODIS images in Southeastern Germany exhibiting that LST has an effect on vegetation health indices including VCI, TCI, NDVI, and VHI. In the case of the climate change effect on vegetation, LST and its correlation with drought indices, the following studies have been carried out. Gidey *et al*. (2018) analyzed the duration, onset, frequency, cessation, density and spatial extent of agricultural drought using drought indices including LST, VCI, TCI, DVI, and VHI in northern Ethiopia from 2001 to 2015 reporting that the NDVI index decreased by 3-4% during the main rainy season in all regions of the study area, while the LST index indicated a significantly elevation of 0.52-1.08 °C. The amount of Vegetation Health Index (VHI) decreased significantly during the main rainy season. In addition, Masitoh & Rusydi, (2019) examined the VHI, LST and NDVI indices from 2008 to 2017 in the dry season of the Brantas watershed reporting that LST has a high effect on the vegetation dryness in this watershed. Moreover, Kouroumaa *et al*. (2021) investigated drought indices including NDVI and VCI in the productivity of agricultural products in Ethiopia using Landsat-8 satellite images from 2003 to 2019. Their finding revealed that the greatest agricultural drought occurred in 2003, 2004, 2008, 2009 and 2015. Harishnaika *et al*. (2022) surveyed drought indices such as LST, VCI, TCI, VHI, and NDVI using Landsat-8 satellite images and GIS technique in the semi-arid areas of Karnataka State in 2015-2019 reporting that the highest percentage of severe agricultural

drought occurred in the northeast of Chinthamani taluk with an area of 740.20 km^2 (20%). Furthermore, Del-Toro-Guerrero *et al.* (2022), checked drought meteorology on areas covered by natural ecosystems in the Guadalupe Watershed of Mexico using TM, ETM$^+$ sensors of Landsat 7 and OLI/TIRS Landsat 8 and drought indices included VHI, NDVI, LST, and NDWI. Their findings indicated that the Guadalupe region was affected by drought more than 87% during 2001, 2006, 2013 and 2017 and also revealed that there is a relationship between the VHI index and the LST, which helps us to predict the LST (Gidey *et al*. 2018). Zhang *et al*. (2019) stated that seasonal and interannual drought events can be shown using VCI and TCI indices, since both indices can help estimate VHI (Rhee *et al*. 2010). The purpose of the present study was to investigate the climate change effects on the ecosystem services such as TA regulation, LST and drought reduction and assessing the spatial distribution of Tajan watershed drought from 2013 to 2023 using Landsat 8 OLI sensor images. So, satellite indices can be used in the absence of meteorological indices for drought monitoring studies.

MATERIALS AND METHODS

Study Area

The Tajan watershed with an area of 4015.88 Km^2 is located at 53º 04' 57" to 53º 18' 26" longitude and 36º 09' 17" to 36º 29' 49" latitude in North Iran (Fig. 1). The average annual temperature is 15 ℃, and a mean rainfall of 630 mm per year. The Sefidroud, Chahardangeh, Zalamroud, and Tajan rivers are located in the watershed. Tajan River is the largest river in the watershed which originates from a height of 3251 meters at the Hezar Jarib Mountains on the northern slope of the Alborz Mountain in the south of Sari City. It shares boundaries with the Caspian Sea in the north, the Darabkala and Nakaroud River in the east, the Semnan Province in the south, and Siahroud and the Talar rivers in the west. The length of the main branch of the river is 172 km, which passes through Sari City to the Caspian Sea (RWCM, 2022).

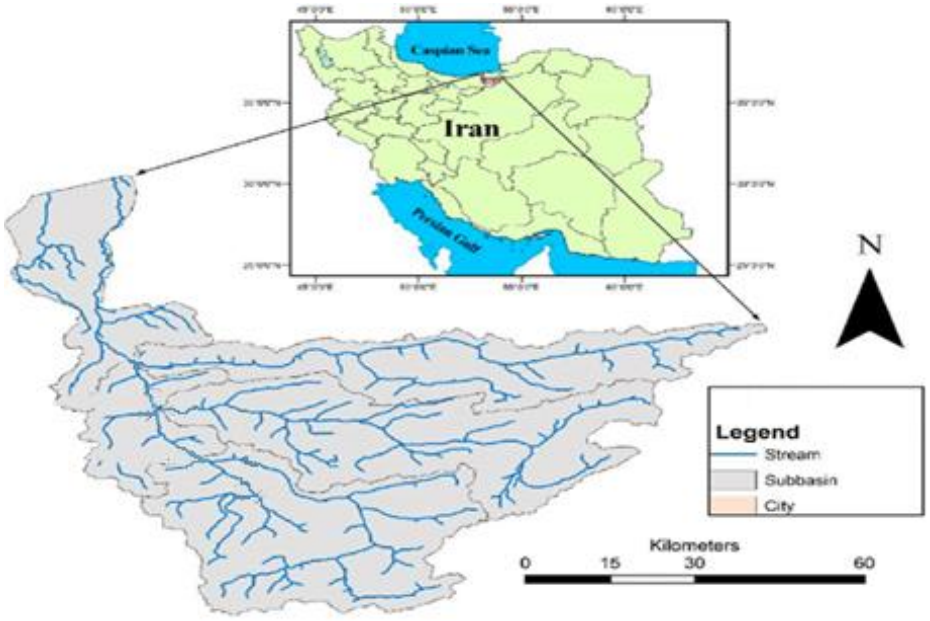

Fig. 1. Geographical location of Tajan watershed.

In this study, Landsat 8 OLI satellite images were used to evaluate the Tajan watershed ecosystem services from 2013 to 2023. Landsat 8 OLI satellite images were downloaded from the website of the United States Geological Survey (USGS). For choosing the period time of the satellite images, an effort was made to choose images from one season with a short time interval between downloaded images. Also, the land cloud cover of satellite Landsat images is close to zero (Kong *et al*. 2019, Del-Toro-Guerrero *et al*. 2022, Pourhabib *et al*. 2025). Since the LST and the state of vegetation cover of the Tajan watershed reaches their maximum from July to September, Landsat satellite images were monitored during these months. Then, the image was subset in the ENVI5.3 software based on the boundary of the Tajan watershed. In addition, for reducing the errors of images, geometric and radiometric corrections were done in the ENVI software. Table 1 indicate the image specifications used in the research. For investigating the climate change effects on the air Temperature (Ta) regulating, Land Surface Temperature (LST) and drought reduction in Tajan watershed, drought indices such as LST Index, Vegetation Condition Index (VCI),

Vegetation Health Index (VHI), Temperature Condition Index (TCI), Soil Adjusted Vegetation Index (SAVI), and Normalized Difference Vegetation Index (NDVI) were calculated as follows.

Table 1. The images specifications.

Date	Path	Row	Year
2013-07-07	35	163	2013
2014-07-26	35	163	2014
2015-08-14	35	163	2015
2016-06-29	35	163	2016
2017-09-20	35	163	2017
2018-09-07	35	163	2018
2019-09-26	35	163	2019
2020-09-12	35	163	2020
2021-08-30	35	163	2021
2022-09-18	35	163	2022

Land surface temperature (LST)

LST is one of the factors that have attracted researchers' attention in drought studies. The LST is closely related to vegetation cover, its density and soil moisture (Zaharaddeen *et al*. 2016; Zuhro *et al*. 2020). According to previous studies, for producing the LST index map, it is necessary to have thermal bands that have low resolution and are available to researchers for a long time (Karnieli *et al*. 2019b). Therefore, to estimate the LST, various methods such as Mono-Window Algorithm (MWA), Split Window (SW), Single-Channel Method (SCM), Qian's Split-Window Algorithm (SWA-Q), Sobrino's Split-Window Algorithm (SWA-S), and the Surface Energy Balance Algorithm for Land (SEBAL) Algorithm, etc., were used. However, based on the results of previous studies, the split window method is more suitable than other methods for calculating the LST. Therefore, in this study, the split window algorithm was used to estimate the LST index. To extract the LST index, we used band 10 of the OLI sensor images. For calculating the index, the digital numbers of their images were converted to spectral radian (Lλ) using Eq. 1. Then, the Brightness Temperature (TB) was calculated using Eq. 2 (Ibrahim & Abu-Mallouh 2018).

$$L\lambda = \frac{Lmin - Lmax}{Qmax - Qmin} \times (DN - Qmin + Lmin) \quad \textbf{(1)}$$

$$TB = \frac{K_2}{ln(\frac{K_1}{L\lambda} + 1)} \quad \textbf{(2)}$$

In Eq. 1, L_{max} and L_{min} indicate the maximum and minimum radiance values of the thermal bands, and Q_{max} and Q_{min} show QUANTIZE_CAL_MAX_BAND_10 and QUANTIZE_CAL_MIN_BAND_10 values respectively, which are equal to 65535 and 1. Furthermore at the Eq. 2, TB is the effective temperature in the satellite is based on Kelvin; K_1 and K_2 are satellite-specific constants; K_1 is the first thermal calibration constant; K_2 is the second thermal calibration constant, and Lλ is the spectral radiance of the pixel. For Landsat 8, the values K_2 and K_1 are 1321.0789 and 774.8853, respectively. The values of these factors were extracted from the images Metadata file (MTL; Bastiaanssen *et al*. 1998).

In the algorithm, Fractional Vegetation Cover (FVC) was calculated using Eq. 3, and the Normalized Difference Vegetation Cover Index (NDVI) was estimated using Eq. 6 (Sobrino *et al*. 2004).

$$FVC = (\frac{NDVI - NDVImin}{NDVImax - NDVImin})^2 \quad \textbf{(3)}$$

Additionally, the value of Land Surface Emissivity (ε) was estimated using Eq. 4 (Markham & Barker 1985). Finally, the Land Surface Temperature (LST) was obtained using Eq. 5 (Eze *et al*. 2020).

$$\varepsilon = 0.004FVC + 0.986 \quad \textbf{(4)}$$

$$LST = \frac{BT}{1 + W(\frac{BT}{P}) + LN\,\epsilon} \quad \textbf{(5)}$$

In Eq. 5, LST is the land surface temperature based on degrees Celsius (°C), W is radiance wavelength (11.5 μm), p: constant coefficient (1.438×10^{-2} mk). The values of these factors are extracted from the MTL file.

Normalized Difference Vegetation Index (NDVI)

NDVI is widely used to distinguish areas with healthy vegetation from unhealthy and areas without vegetation cover (Karnieli *et al*. 2019a). NDVI indicates the vegetation status on the wide surface areas (Xiao *et al*. 2014). The numerical value of the NDVI varies between -1 and +1. Positive numerical values related to dense vegetation and numerical values of zero and values close to zero correspond to areas without vegetation and the negative values of the index (numbers close to -1) indicate water areas. NDVI was calculated according to the reflection values of the red and near-infrared bands. NDVI was estimated using Eq. 6 (Kogan & Guo 2016). Red and NIR (near infrared) in Eq. 6 are bands 4 and 5 of the OLI sensor.

$$NDVI = \frac{NIR-RED}{NIR+RED} \quad \textbf{(6)}$$

After calculating the NDVI, other drought indices including Vegetation Health Index (VHI), the Vegetation Condition Index (VCI), Temperature Condition Index (TCI), and Soil Adjusted Vegetation Index (SAVI) were calculated in the Tajan watershed from 2013 to 2023. Therefore, each of the mentioned indexes are calculated using the visible and thermal bands of the Landsat, the OLI Landsat 8 sensor images, and the following equations.

Soil Adjusted Vegetation Index (SAVI)

In areas where the vegetation cover is low-density and so-called thin, the soil reflection impact affects the vegetation reflection effect (Möllmann *et al*. 2019). The SAVI is the corrected NDVI. The index reduces the effects of soil surface and soil moisture in the NDVI. SAVI was calculated using Eqs. 7, 8, and 9:

$$SAVI = \frac{(1+L)(NIR-RED)}{L+(NIR+RED)} \quad \textbf{(7)}$$

$$L = 1 - 2a \times NDVI \times WDVI \quad \textbf{(8)}$$

$$WDVI = NIR - RED \quad \textbf{(9)}$$

In the above equations, L is the soil effects correction factor with values between 0 and 1 (The closer this index value is to 1, the denser the vegetation cover is more). The L factor is calculated using Eq. 8, where a = 1.6 and γ is the soil line coefficient (Somvanshi & Kumari 2021).

Vegetation Status Index (VCI)

Previous studies showed that the NDVI was a suitable index to identify plant stress and damaged crops (Mishra & Singh 2011). Since in areas with heterogeneous land cover the difference between the surface and vegetation amount depends on factors such as the vegetation type, climate and soil type, hence the NDVI performance faces limitations in heterogeneous areas (Huang *et al*. 2021). The NDVI has two components: ecology and climate (He *et al*. 2021). Estimating weather effects on vegetation cover is possible only after removing effects related to geographic parameters containing climate, soil, and topography. The climate component which shows the health and greenness of the plant is related to parameters such as precipitation (Kloos *et al*. 2021). Therefore, Kogan (1990) introduced the VCI for estimating the weather effects on vegetation. In this way, the maximum and minimum long-term NDVI values are determined for each pixel in the month and used in the VCI equation (Eq. 10). Previous studies have shown that the VCI provides a better performance than the NVDI in assessing drought, particularly in geographically heterogeneous regions (Zambrano *et al*. 2016). The VCI was calculated using Eq. 10:

$$VCI = \frac{NDVIj-NDVI_{min}}{NDVI_{max}-NDVI_{min}} \quad \textbf{(10)}$$

In Eq. 10, $NDVI_j$, $NDVI_{max}$, and $NDVI_{min}$ are the normalized vegetation difference indexes of the study area, the minimum and maximum value of the NDVI respectively and j is the andis of the month (Zambrano *et al*. 2016). Therefore, if the VCI approaches zero, it indicates a severe drought rate in that month, and a high VCI value shows vegetation health (Gidey *et al*. 2018).

Temperature Condition Index (TCI)

TCI is similar to the VCI that was proposed by Kogan in 1995. It was introduced by normalizing the LST index (Gidey *et al*. 2018). The index was estimated using Eq. 11 (Gidey *et al*. 2018). In this regard, LST is Land Surface

Temperature; LST_{max} and LST_{min} are the maximum and minimum LST in a specific period time in the long term respectively. The TCI value changes between 0 and 1, which is close to zero under drought conditions and close to one under wet periods (Karnieli *et al*. 2006).

$$TCI = \frac{LST_{max} - LST}{LST_{max} - LST_{min}} \quad \textbf{(11)}$$

Notably, VCI was created according to the relationship between the actual NDVI value and the NDVI values in the best and worst humidity conditions of the plant growing season. While the TCI is based on the correlation between the actual LST and the temperature of potential conditions (LST_{min}) and plant stress (LST_{max}). According to the drought effects on vegetation and surface temperature, VCI and TCI were created based on NDVI and LST time series data (Gidey *et al*. 2018).

Vegetation Health Index (VHI)

As previously mentioned, TCI and VCI show the temperature and humidity conditions of the vegetation, respectively. Kogan (1995) by introducing the VHI showed Vegetation Health Index is a combination of Vegetation Status Index and Temperature Condition Index, which aims to use vegetation moisture conditions and ground surface temperature in an index during drought stress (Möllmann *et al*. 2019). In the present research, the Vegetation Health Index was calculated using Eq. 12 (Chang *et al*. 2021).

$$VHI = r_1 \times VCI + r_2 \times TCI \quad \textbf{(12)}$$

In Eq. 12, factors r_1 and r_2 are the weight of VCI and TCI respectively. Since the contribution of humidity and temperature during the vegetation cycle is normally uncertain, the contribution of VCI and TCI in VHI is considered equal (Chang *et al*. 2021).

RESULTS AND DISCUSSION

The finding of the assessment of the climate change effect on the Tajan watershed drought using the Landsat 8 OLI satellite images and drought indices are as follows:

Land Surface Temperature (LST)

The findings of LST in the Tajan watershed indicated that the Land Surface Temperature index had an increasing trend from 2013 to 2022 (Fig. 2). So that the minimum LST index value increased from 15.7 ℃ in 2013 to 24.2 ℃ in 2016; and then from 8.42 ℃ in 2017 to 17.7 ℃ in 2022. In other words, during the 10 years, 8 ℃ has been added to the LST (Fig. 2). The result of the minimum and maximum LST index values during different years has been indicative of climate change in Tajan watershed. The finding of the investigation of LST maps showed that the maximum LST from 2013 to 2022 was at the central, eastern, and south eastern parts of Tajan watershed (Fig. 2). In other words, the maximum LST index value was in the classes with low vegetation cover (Minimum NDVI value). Also, matching the LST map with the land use map of Tajan watershed showed that the highest LST value was in residential, barren and unvegetated areas, since in residential areas, the surface of soil, asphalt and cement heat up earlier than other surfaces and absorb heat (Wang *et al*. 2019). Morabito *et al*. (2016) and Shi *et al*. (2017) stated that there is a strong correlation among the NDVI (index value and LST value changes), and the reduction of vegetation cover and the increase of residential and barren areas causes an elevation in LST value. The findings are consistent with the research results. Also, the lowest LST value was observed in the northern and southwestern parts of Tajan watershed. The existence of forest lands, agriculture, and gardens in these areas has reduced the LST in these areas. The finding indicated that vegetation cover can decrease the amount of heat stored in the soil and land surface through transpiration. The result is consistent with the finding of Kayet *et al*. (2016).

Normalized Difference Vegetation Index (NDVI)

To investigate the quantitative and qualitative changes in vegetation cover, the output of the NDVI maps from 2013 to 2022 was classified into four classes. The results showed that the annual changes of NDVI of Tajan watershed had a decreasing trend from 2013 to 2022 (Fig. 3). The maximum NDVI value has reached from 0.7 in 2013 to 0.5 in 2022. Also, evaluating the minimum vegetation cover classes showed that the area of these classes has increased from 2013 to 2022 (Fig. 2). The results indicated the decreasing trend of vegetation cover. The results are following those of Eze *et al*. (2020) and Wang *et al*. (2018).

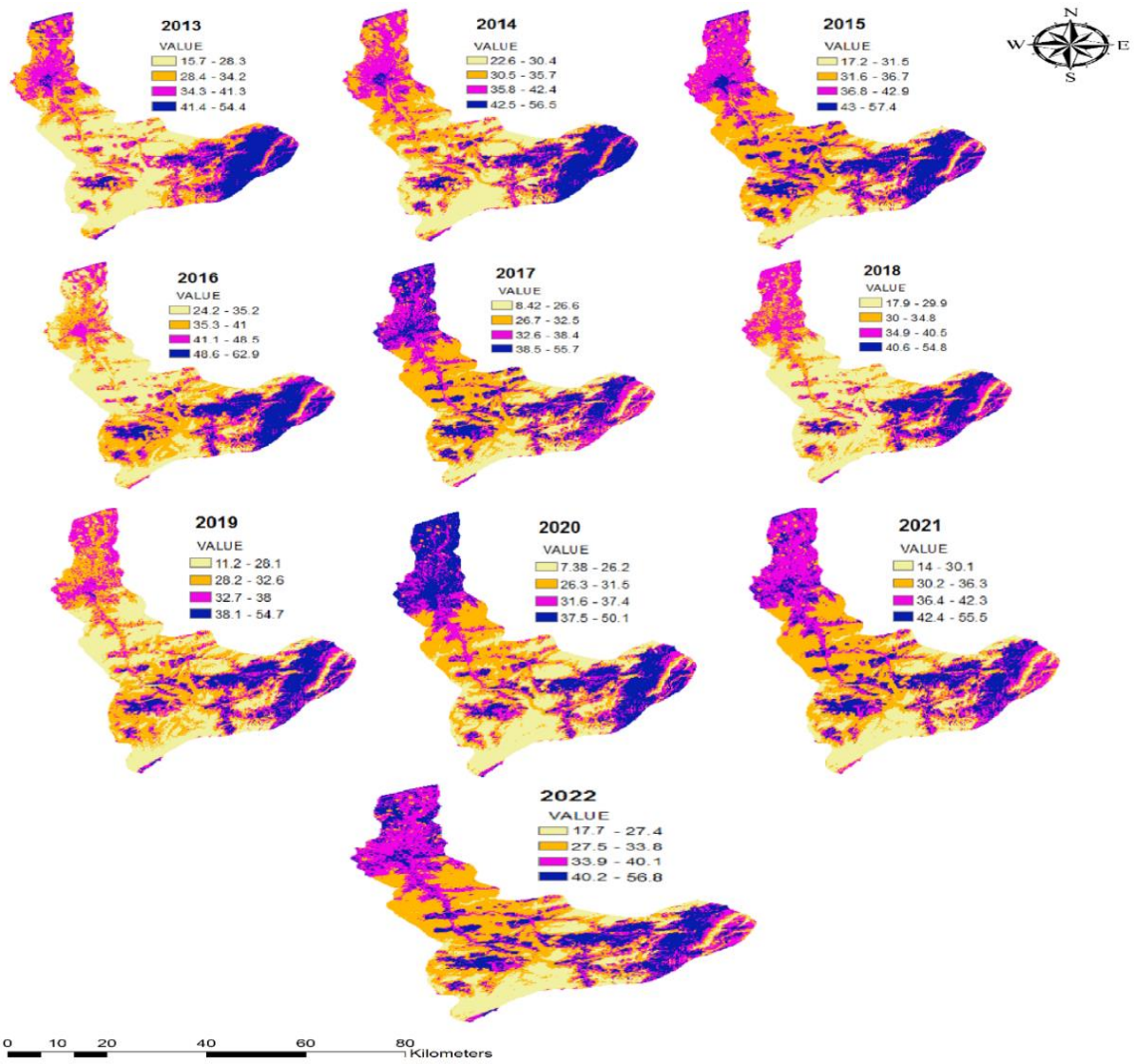

Fig. 2. Spatial and temporal changes of the LST in Tajan watershed.

NDVI map of Tajan watershed is shown that the minimum NDVI value was in the central, eastern, and south eastern parts of the watershed, while the maximum in the northern and southwestern parts from 2013 to 2022 (Fig. 3). The presence of forest lands, pastures, agriculture and gardens in the northern and southwestern parts has increased the NDVI value in these areas. Also, the presence of residential use in the central part of the watershed, and the presence of barren lands without vegetation in the eastern and south eastern direction caused a drop in the NDVI value. Wang *et al*. (2019) findings are consistent with the results of the present study. The results of other indices of drought such as VHI, TCI, VCI, and SAVI are shown in Figs. 4 - 7.

Adjusted Vegetation Index (SAVI)

The investigation map of the SAVI value showed that the amount of the index was different in Tajan watershed (Fig. 4). The value of SAVI depends on the condition and density of vegetation cover in the area. In other words, given the effects of climatic factors (especially rainfall and temperature) on vegetation cover changes, the changes in the SAVI value reflect the effects of climate on the vegetation cover of this area.

The SAVI map showed that the SAVI value has increased from west to east and southeast of Tajan watershed (Fig. 4). The index maximum value reached from one value in 2013 to 0.8 in 2022. The finding of the SAVI value in Tajan watershed showed that in 2017 and 2022 the largest rate of drought occurred based on SAVI due to the elevation in temperature and drop in rainfall (Fig. 10).

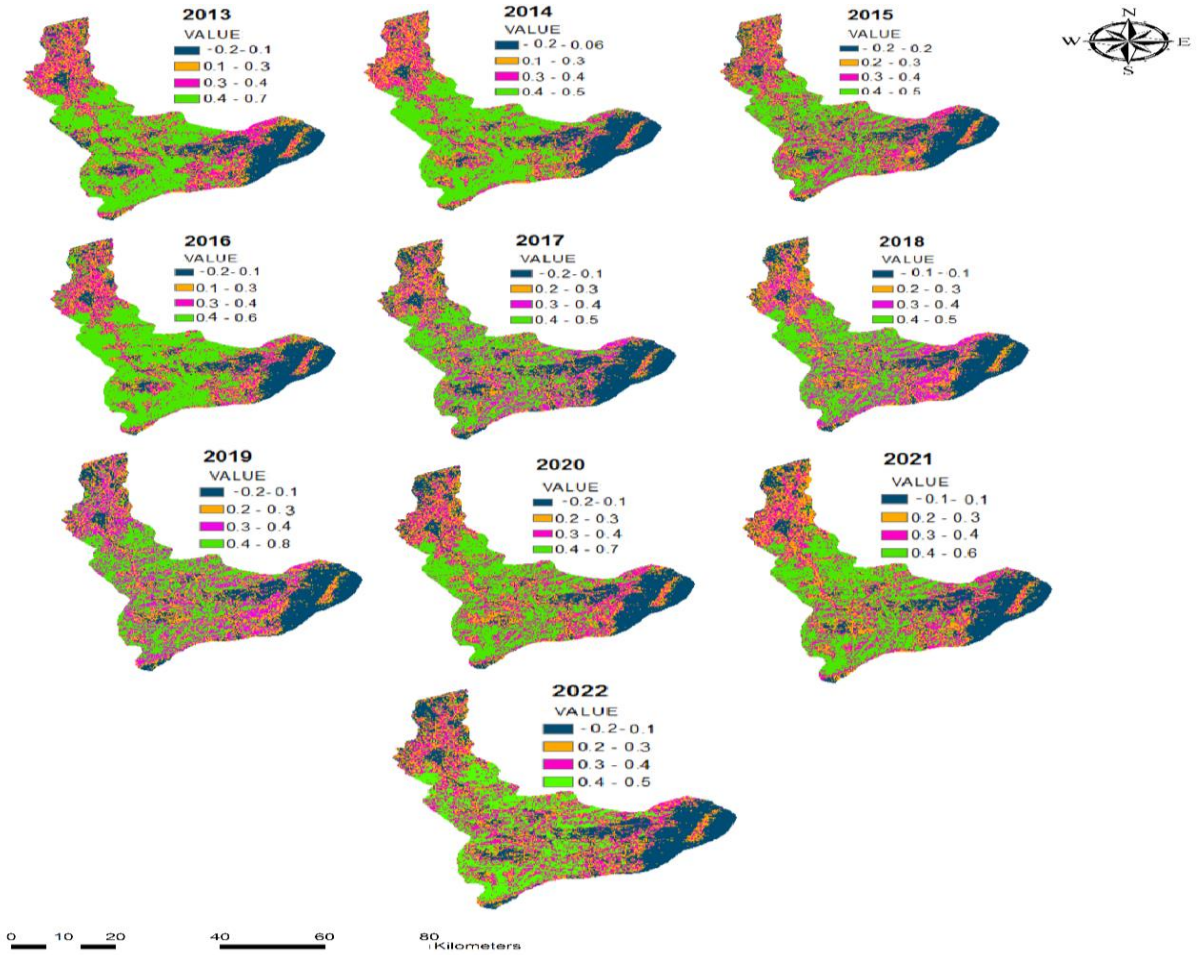

Fig. 3. Spatial and temporal changes of NDVI in Tajan watershed.

Vegetation Condition Index (VCI)

According to the classified VCI map (Fig. 5), there are many changes in the vegetation cover status of Tajan watershed, while the NDVI value was different and had a lower degree, since the VCI map shows that more than 20% of the vegetation cover changed in the watershed (Fig. 4). Based on VCI value from 2013 to 2022, the amount of vegetation cover in Tajan watershed is decreasing and the amount of drought is increasing. Also, based on the VCI value, 2013 to 2016 were the wet years in Tajan watershed.

According to the VCI, large parts of the east and southeast of Tajan watershed have experienced drought with a higher density, and its density has decreased compared to other areas, while experiencing a higher degree of wet in its northern, western, and southwestern areas (Fig. 5). Kouroumaa *et al*. (2021) investigated NDVI and VCI indices in Ethiopia and Harishnaika *et al*. (2022) measured these indices in Chinthamani taluk using Landsat 8 satellite images. Their finding indicated that the highest percentage of agricultural drought in the northeast of the studied areas was due to the drop in rainfall and land use change, which was in consistent with our results.

Temperature Condition Index (TCI)

The results of TCI showed an increasing trend of drought in Tajan watershed from 2013 to 2022 (Fig. 6). Based on the result, large parts of the watershed experienced a higher density of drought in this period. Also, the drought severity was increasing in the eastern, southeastern and north western areas of the watershed (Fig. 6), while the southern and north eastern parts experienced little drought rates. In the present study, the results of TCI and VCI values were different. Liang *et al*. (2017) and Khalil *et al*. (2013) stated that the trends of increasing TCI and VCI values are different once determining the severity of drought.

Vegetation Health Index (VHI)

VHI is widely used in drought monitoring and evaluation (Masitoh & Rusydi 2019). This index can show the effects of drought on both vegetation and surface temperature (Gidey *et al*. 2018). The finding indicated that the drought effects on the vegetation and LST were different. According to the classified Vegetation Health Index (VHI) map, the drought phenomenon was increasing in Tajan watershed (Fig 7). Large parts of the centre and eastern part of the watershed experienced more drought rate, while the severity of drought was decreasing in the northern part (Fig. 7). The result indicated that there is a positive relationship among the VHI and LST alterations. Also, in the central and eastern parts where the LST value was increasing, the VHI value was also elevating. Masitoh & Rusydi (2019), Wang *et al*. (2018) and Kloos *et al*. (2021) stated that there is a correlation between the VHI and LST alterations.

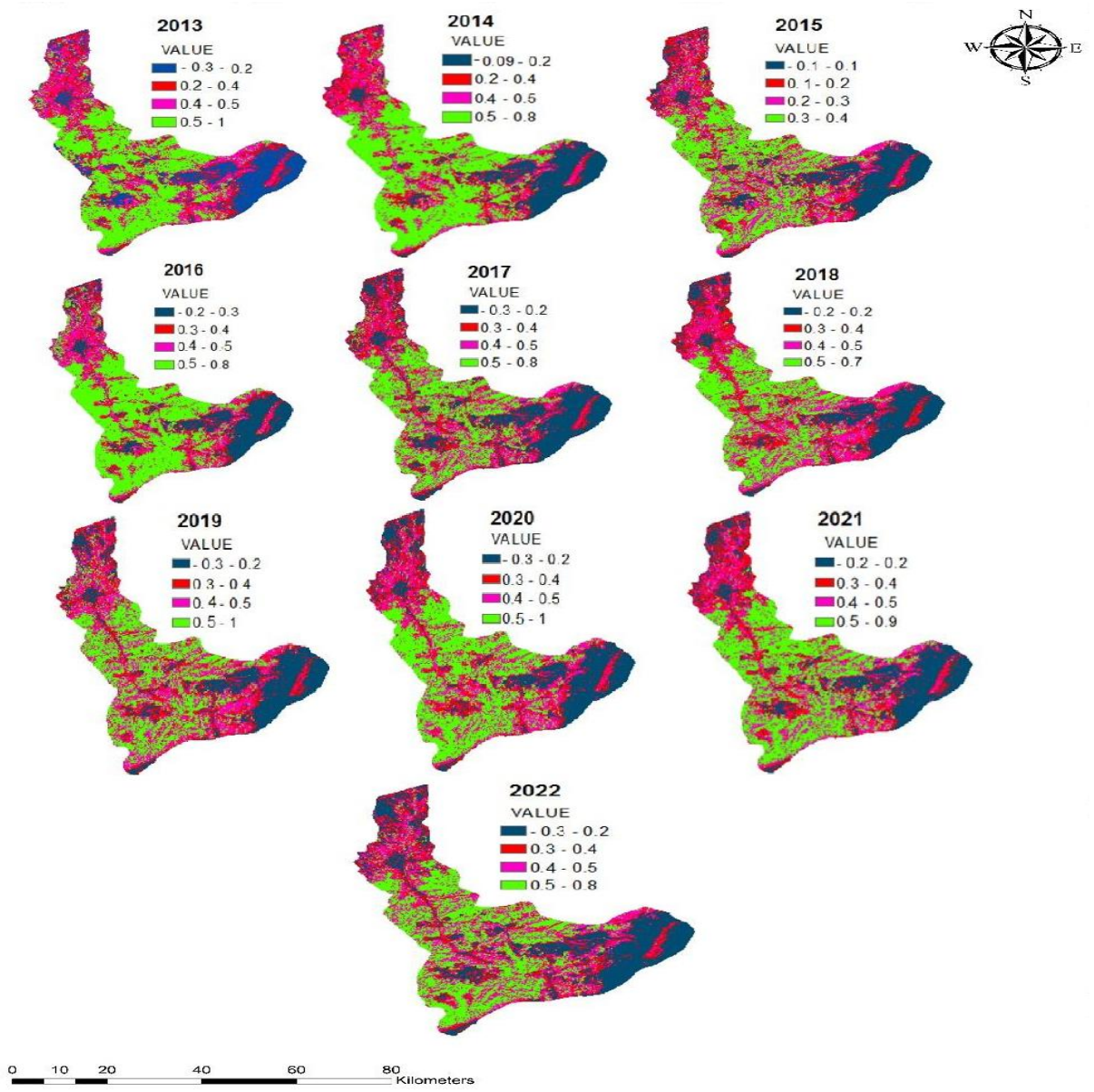

Fig. 4. Spatial and temporal changes of SAVI in Tajan watershed.

The trends of changing in the area of drought classes in Tajan watershed from 2013 to 2023 are shown in Figs. 8-12. According to the LST value, the area of colder classes has always decreased, while that of warmers has elevated during 2013 to 2022 (Fig. 8). In other words, during the last ten years, the warmer classes have been constantly growing. According to the LST index, the highest amount of drought (increasing the land surface

temperature) was observed in 2020. In other words, the area of warm classes upraised during the 10 years (Fig. 8). The trend of changing the area of the NDVI classes during the last 10 years in Tajan watershed showed that the area of the dense vegetation classes has always decreased (Fig. 9). According to the NDVI value, the highest area covered by drought was observed in 2020. Likewise, the highest index value of wet periods was found in 2016.

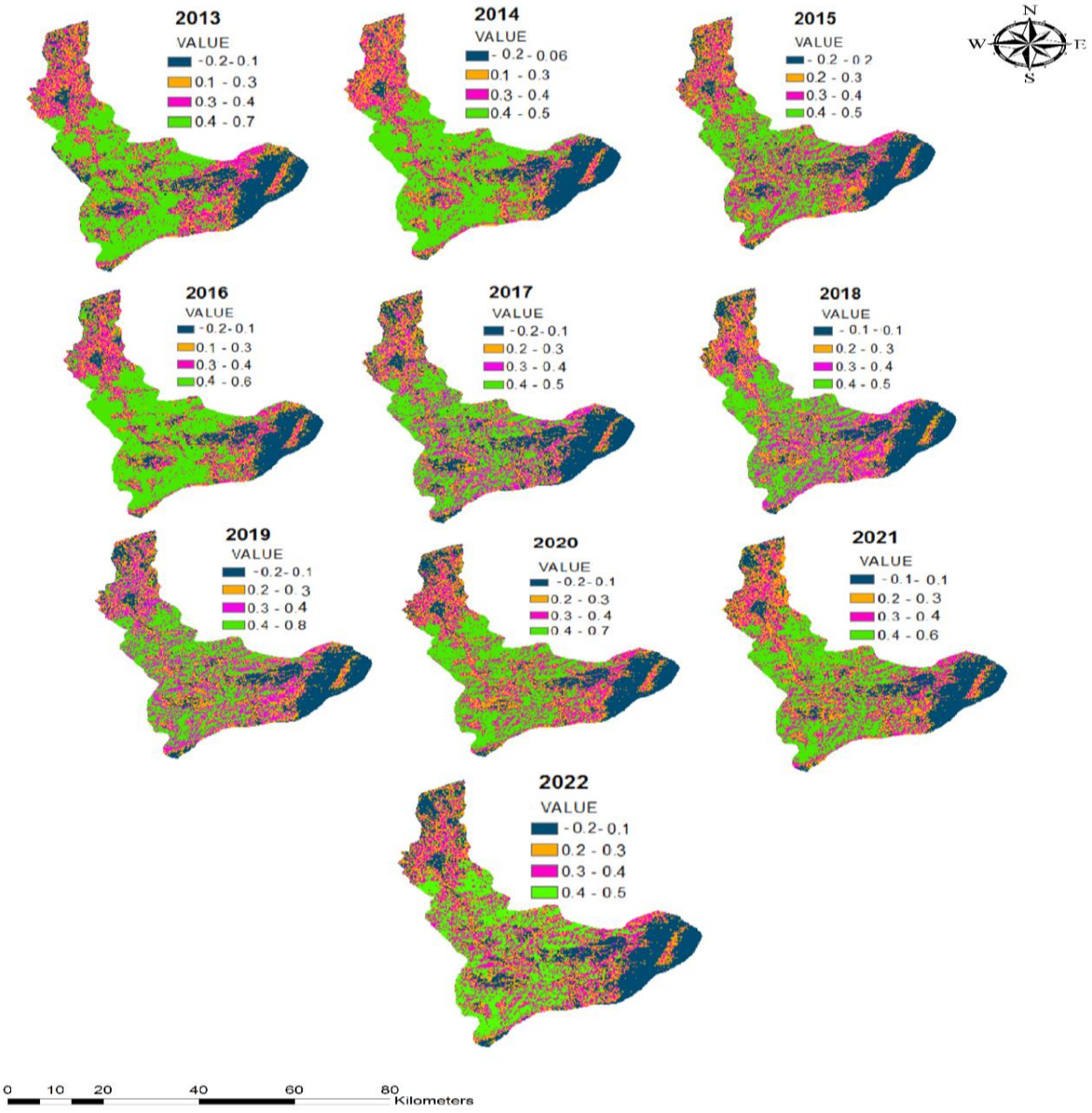

Fig. 5. Spatial and temporal changes of VCI in the Tajan watershed.

The NDVI value from 2013 to 2022 showed that the areas with a rich and high-density vegetation experienced a low land surface temperature value. Since when land's vegetation increases, the surface humidity will be higher and the LST will be lower. Also, the LST value was lower in residential (urban) areas due to the use of asphalt and lack of green space, and in barren lands due to the decrease in the area of vegetation. Much research has been done about correlation between LST and NDVI values. Zhang *et al.* (2018) investigated the correlation among land surface temperature and NDVI values in different land uses, reporting that the human activities have a significant effect on NDVI and LST values. So, the increase in forest and agricultural land will elevate the NDVI value and decline in the LST, since during the processes of photosynthesis and transpiration, green plants absorb

a large amount of heat and CO_2 from the air and causing them to cool down leading to the reduction in the TA and LST. The results indicated a positive correlation among the NDVI value and the degree of drought. The result is consistent with the findings of Kayet *et al*. (2016), who stating that the surface temperature is highly sensitive to vegetation cover and soil moisture, since vegetation cover can reduce the amount of heat stored in the soil through transpiration.

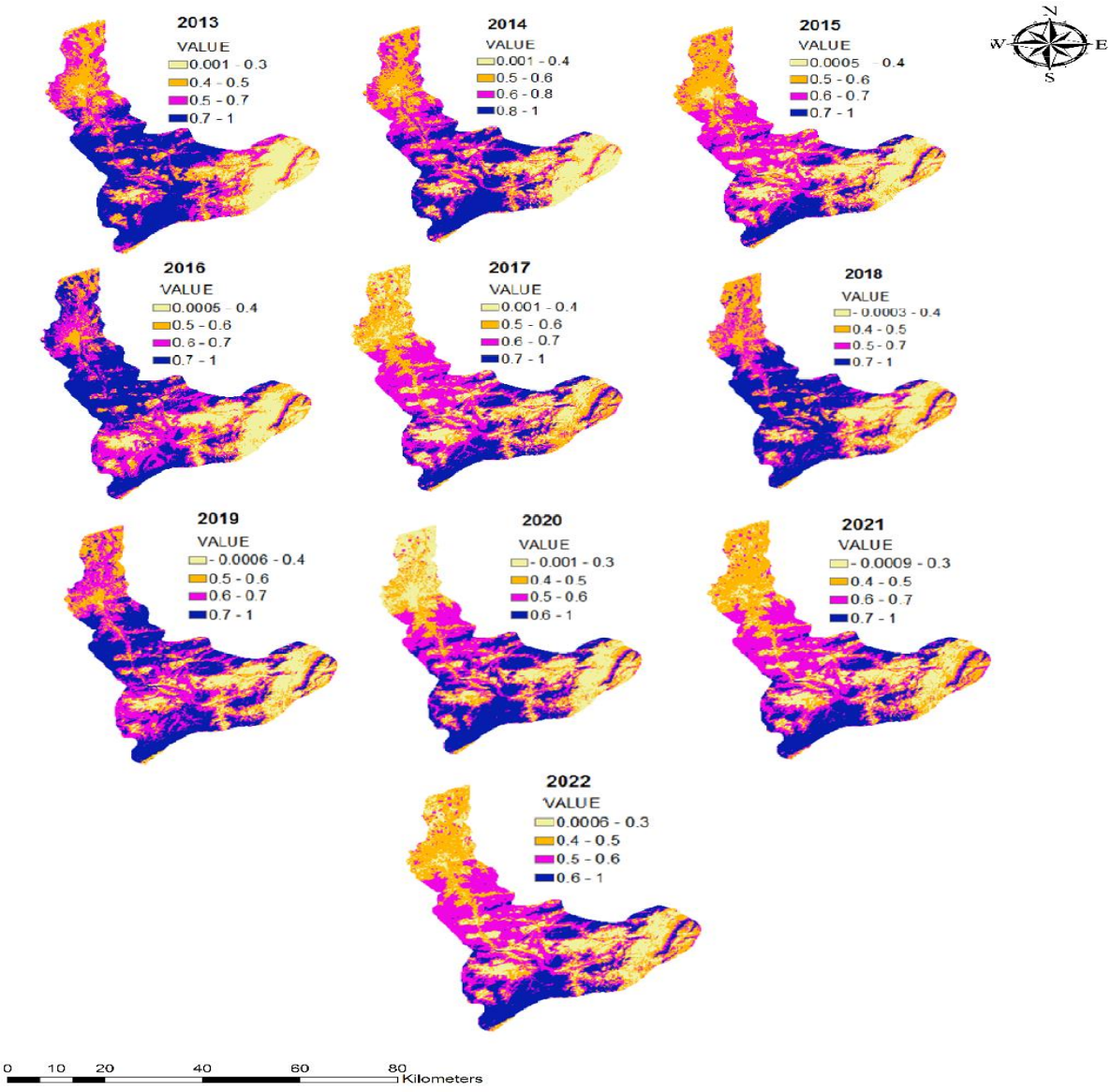

Fig. 6. Spatial and temporal changes of TCI in the Tajan watershed

According to the SAVI values, the highest rate of drought in Tajan watershed occurred in 2017 and 2022, while the highest rate of wet period occurred in 2016 due to the torrential rains in this year. In this regard, Khalil *et al*. (2013) stated that the increasing trend of SAVI value indicates an elevation in the drought severity while a decrease in vegetation cover (Fig. 10). Also, the VCI map showed that the highest rate of drought occurred in 2017 and 2022. In these years, the area under drought has covered 25% of Tajan watershed area (Fig. 11). In this regard, Jiao *et al*. (2016) in the American continent, Zambrano *et al*. (2016) in Biobio Chile, and Pei *et al*. (2018) in China stated that the increasing trend of the VCI value indicate the elevating severity of drought.

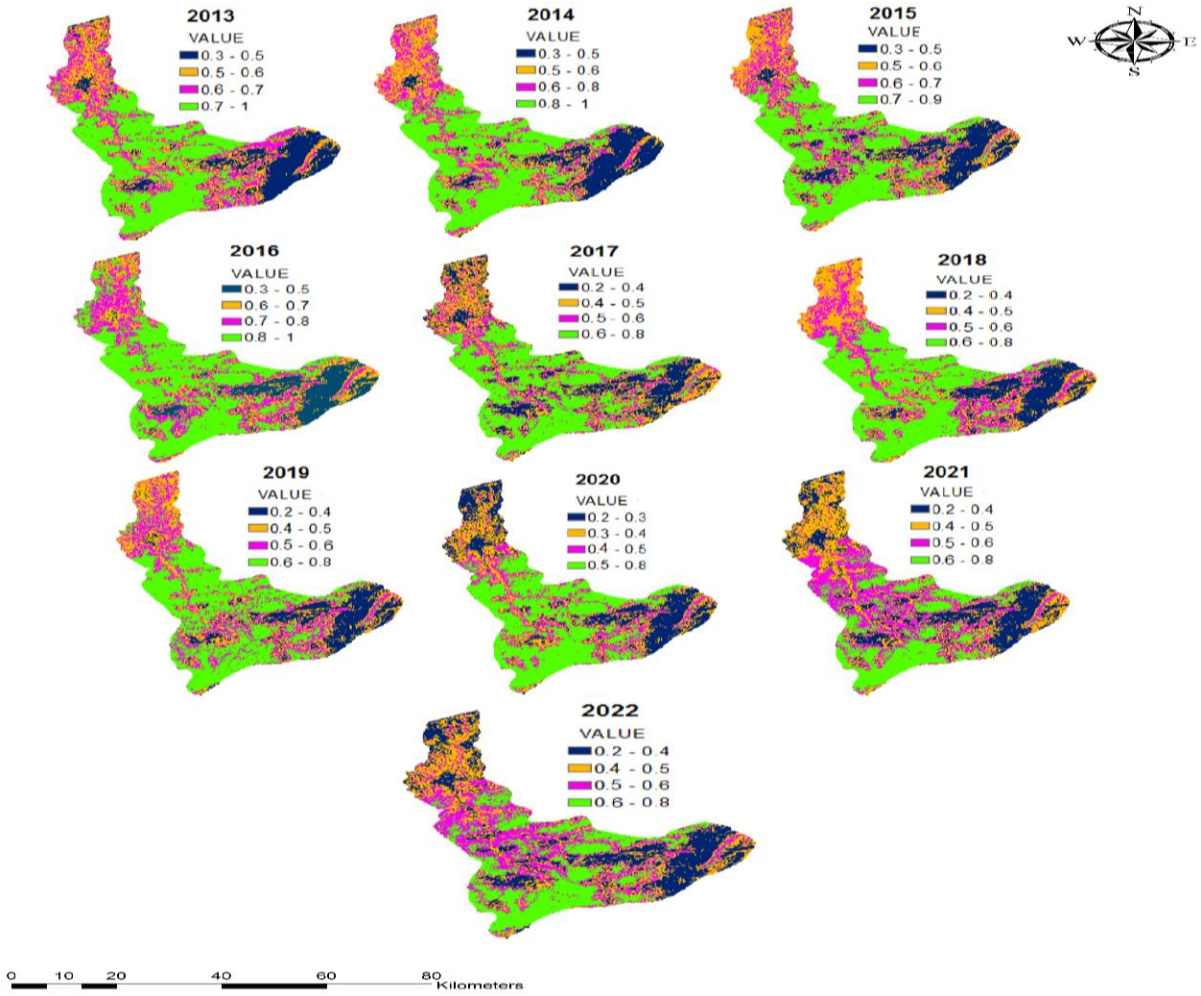

Fig. 7. Spatial and temporal changes of VHI of the Tajan watershed

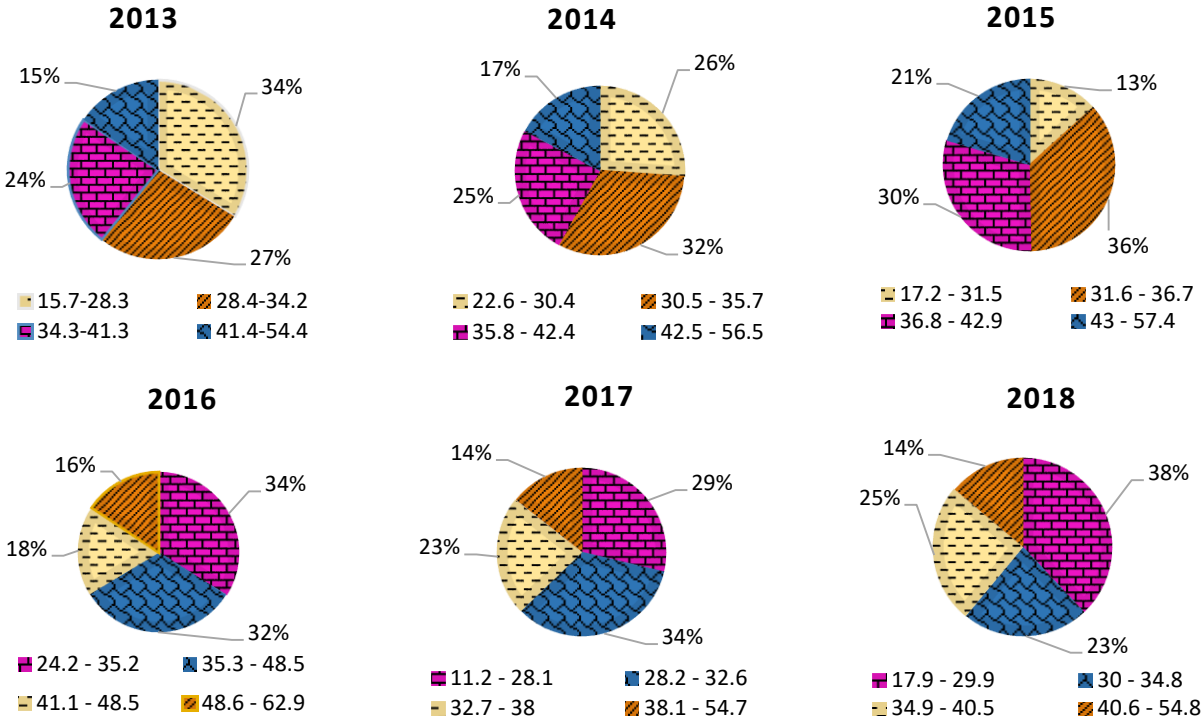

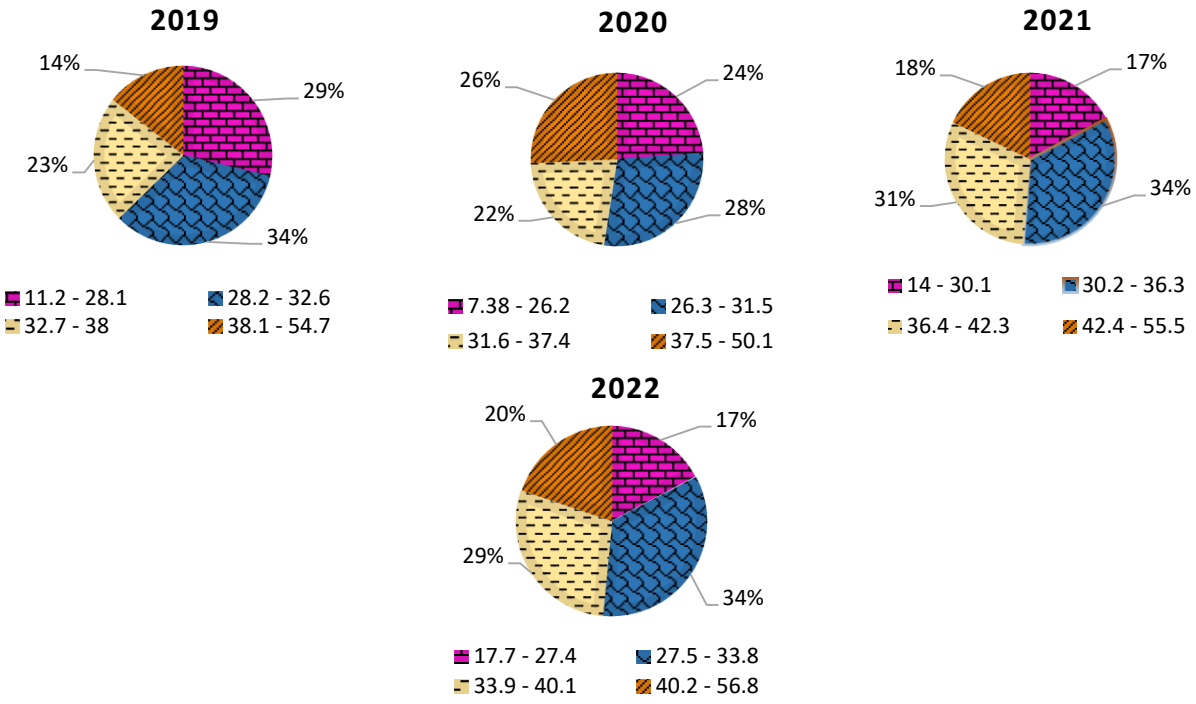

Fig. 8. Percentage of the LST index classes in Tajan watershed.

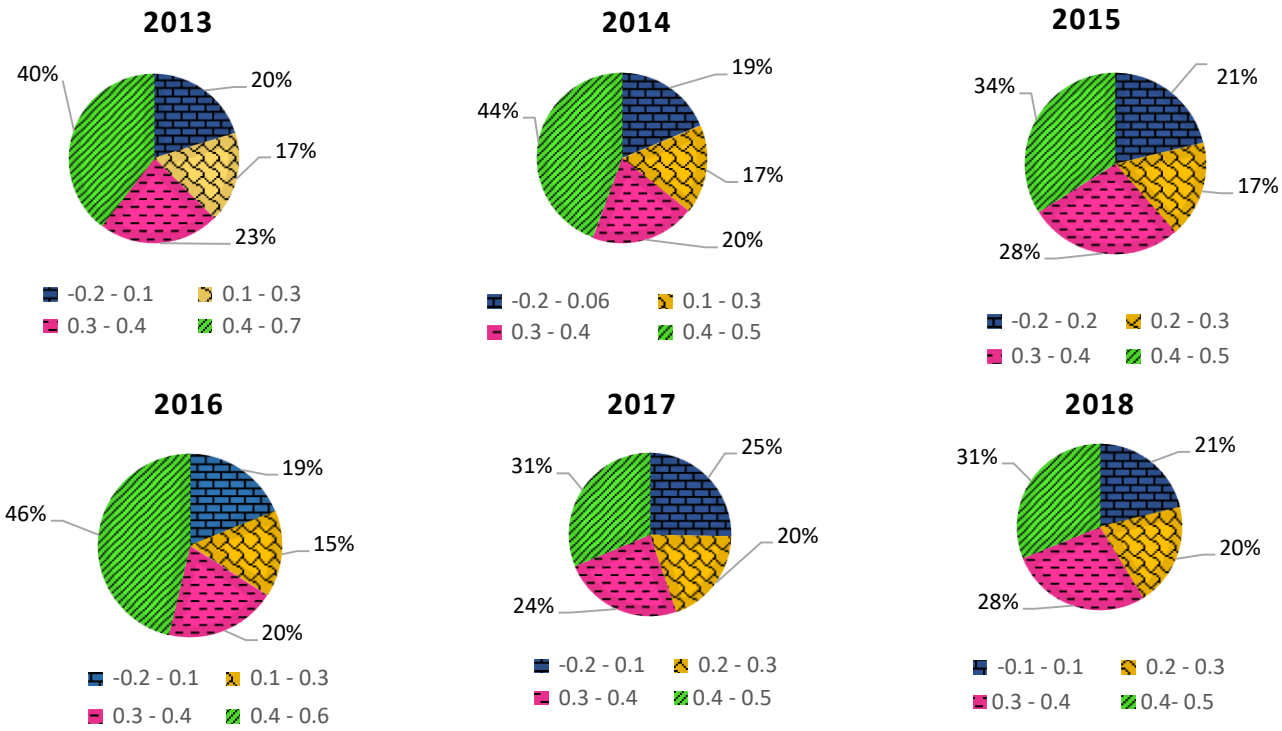

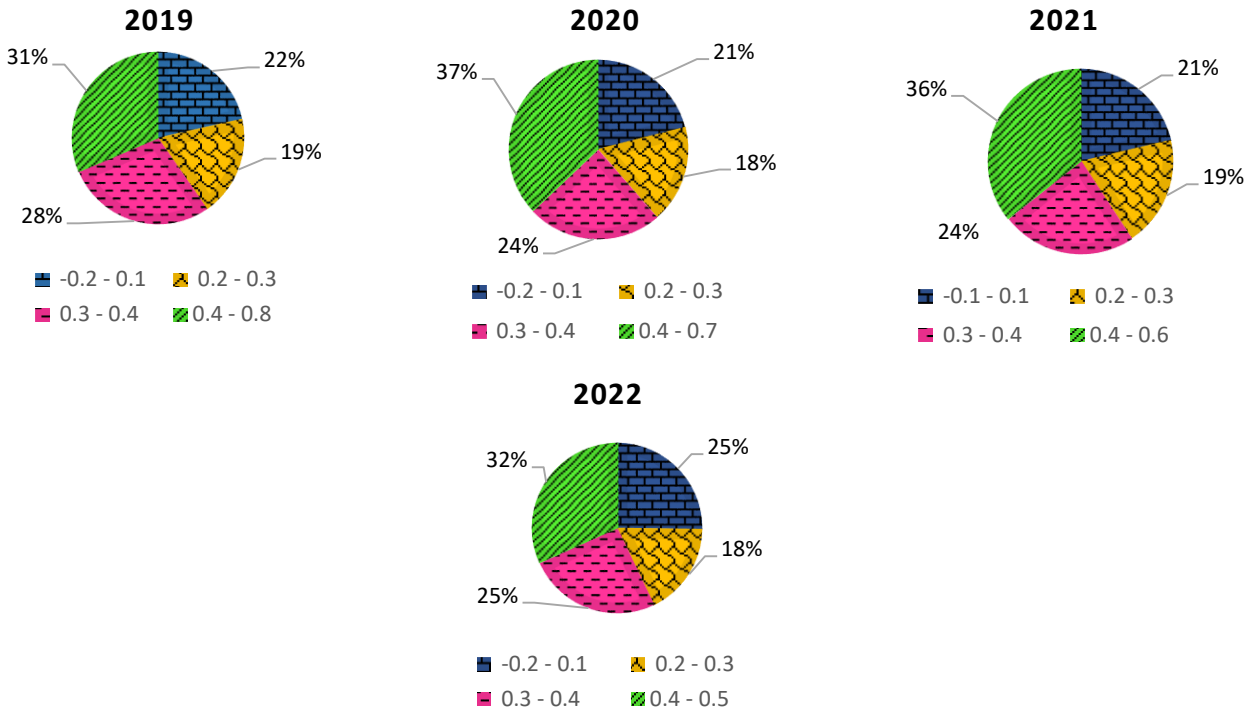

Fig. 9. Percentage of the NDVI classes in Tajan watershed.

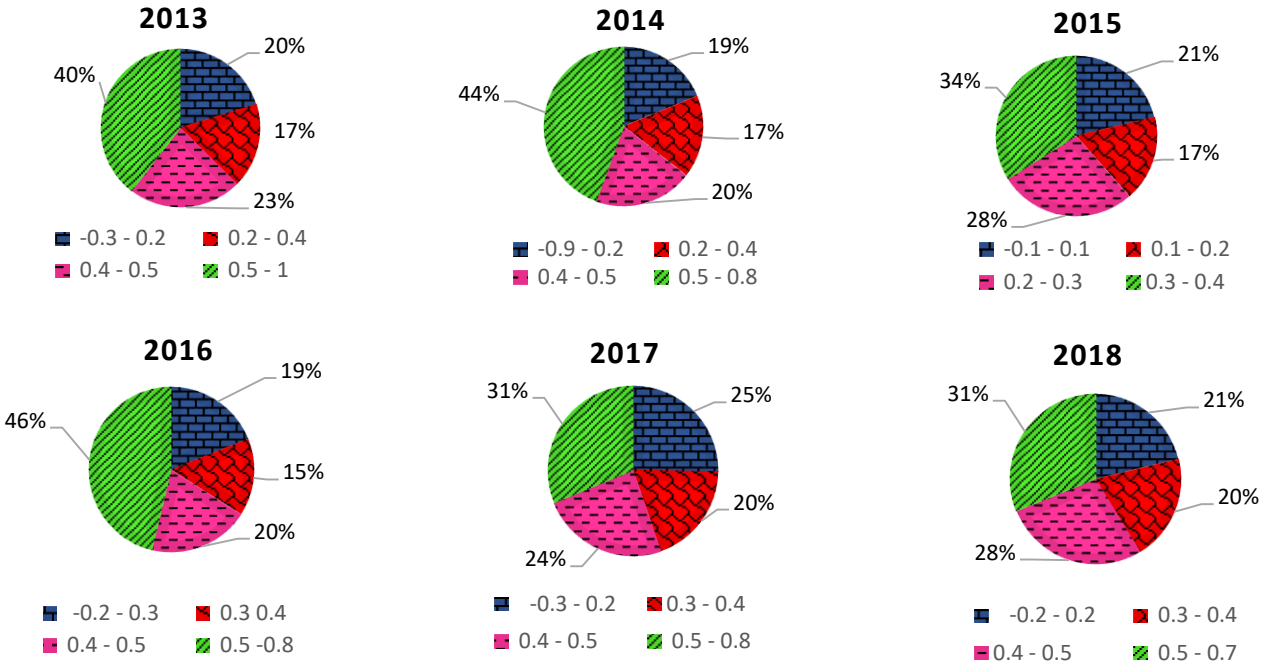

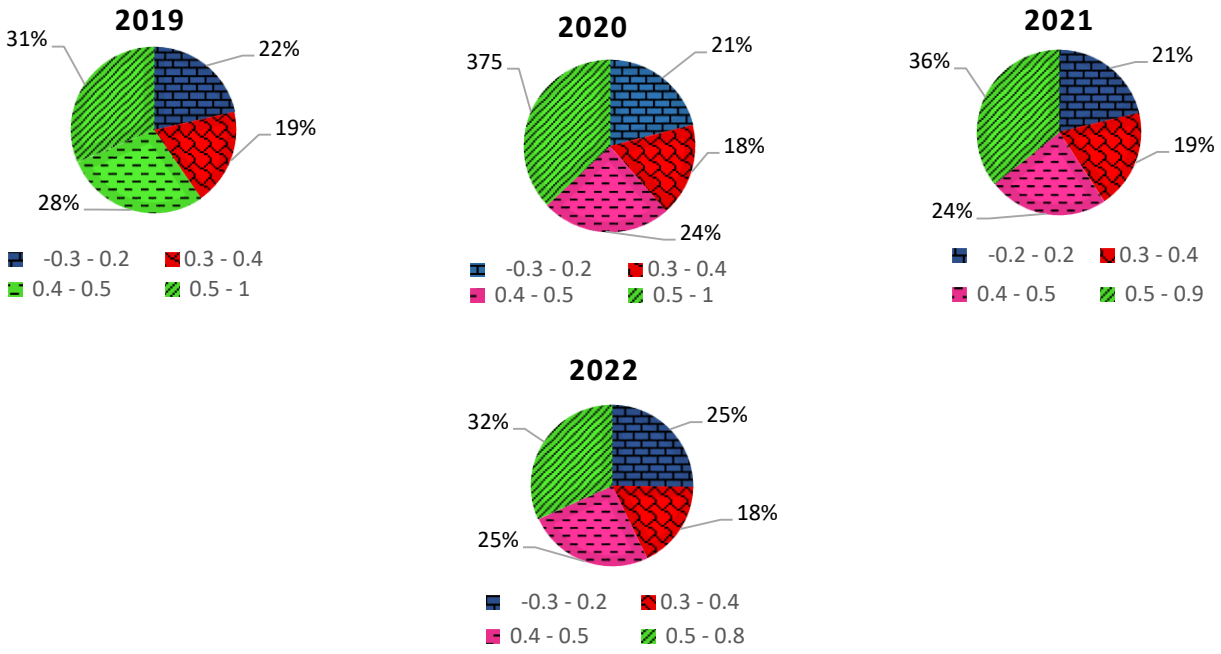

Fig. 10. Percentage of the SAVI classes in Tajan watershed.

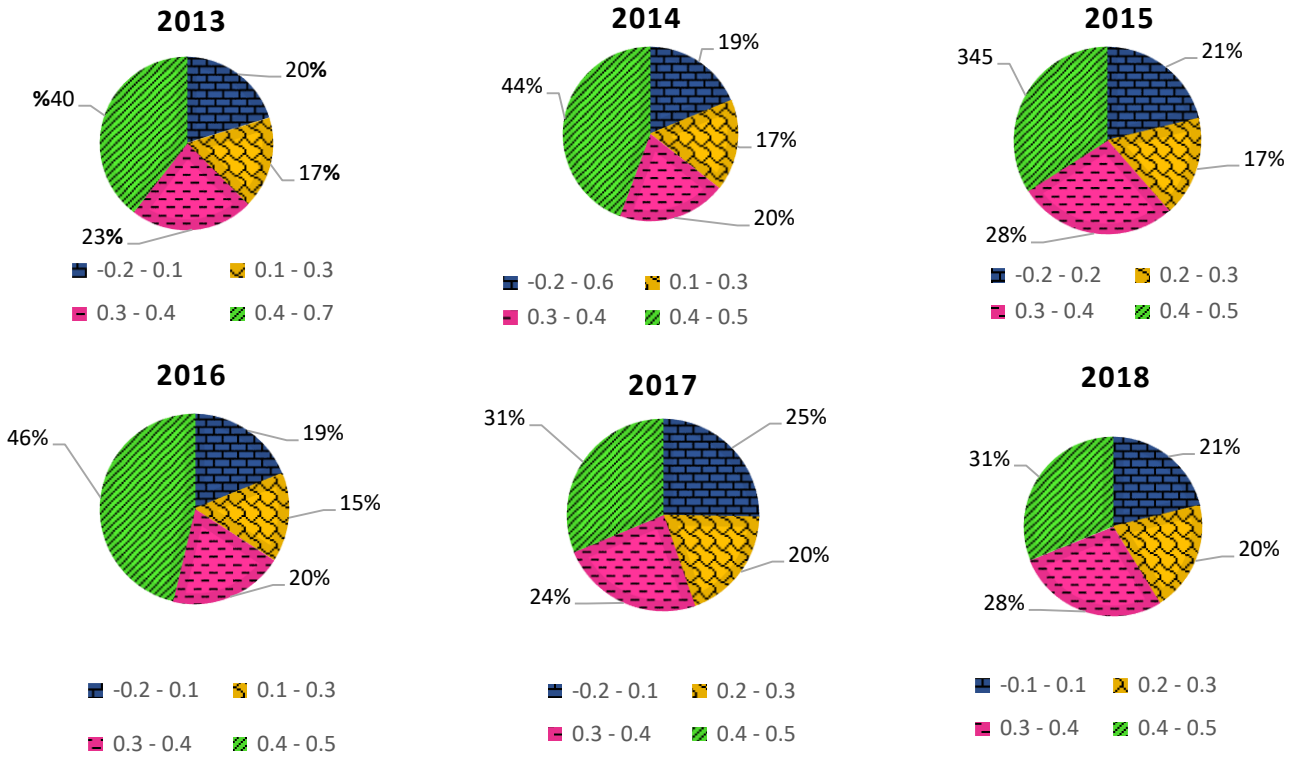

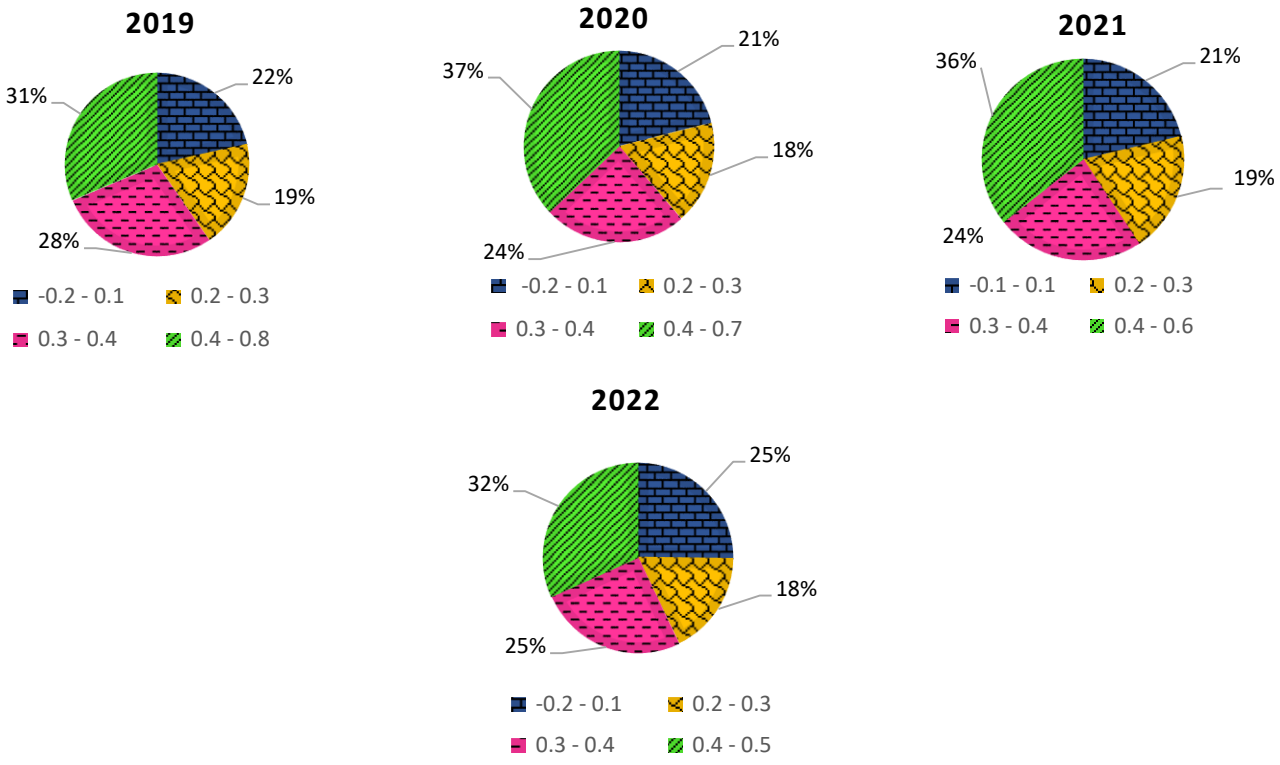

Fig. 11. Percentage of the VCI classes in Tajan watershed.

According to the TCI value, the highest rate (24.04% of Tajan watershed) of drought occurred in 2020. In this regard, Khalil *et al*. (2013) and Pei *et al*. (2018) stated that the increasing trend of TCI value indicates the elevating severity of drought. The percentage of each drought class of Tajan watershed has been calculated using the VHI value for the years from 2013 to 2022 in Fig. 12. The result showed that the highest rate of drought (23.92%) in Tajan watershed occurred in the 0.2-0.4 class in 2022, while the lowest drought in 2016 (Fig. 12). As mentioned earlier, the reason was related to the torrential rains occurred this year. The findings were similar to that of Du *et al*. (2018) and Gidey *et al*. (2018).

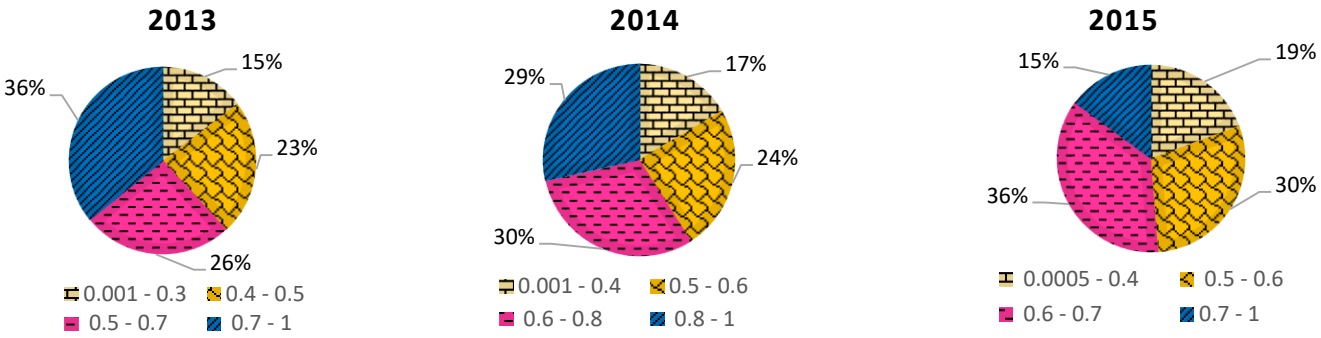

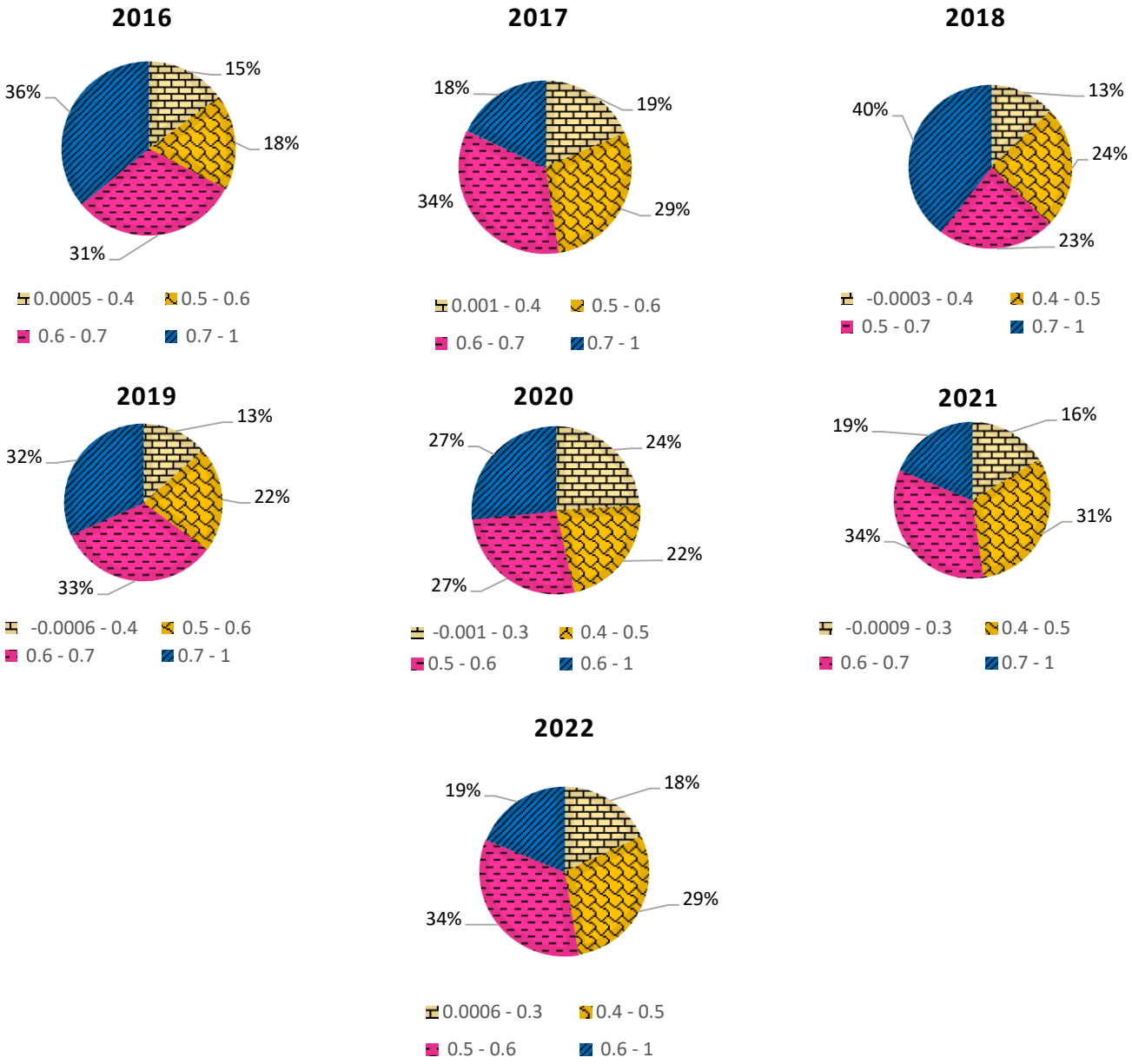

Fig. 12. Percentage of the TCI classes in Tajan watershed.

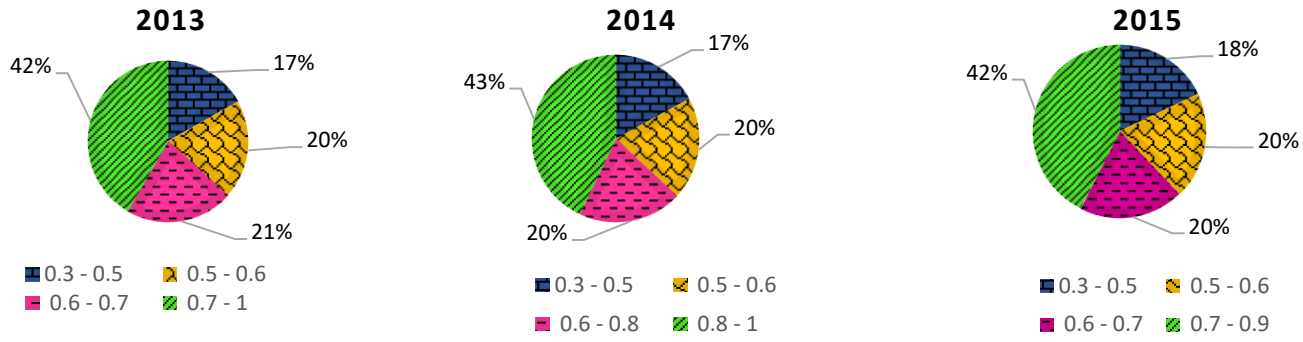

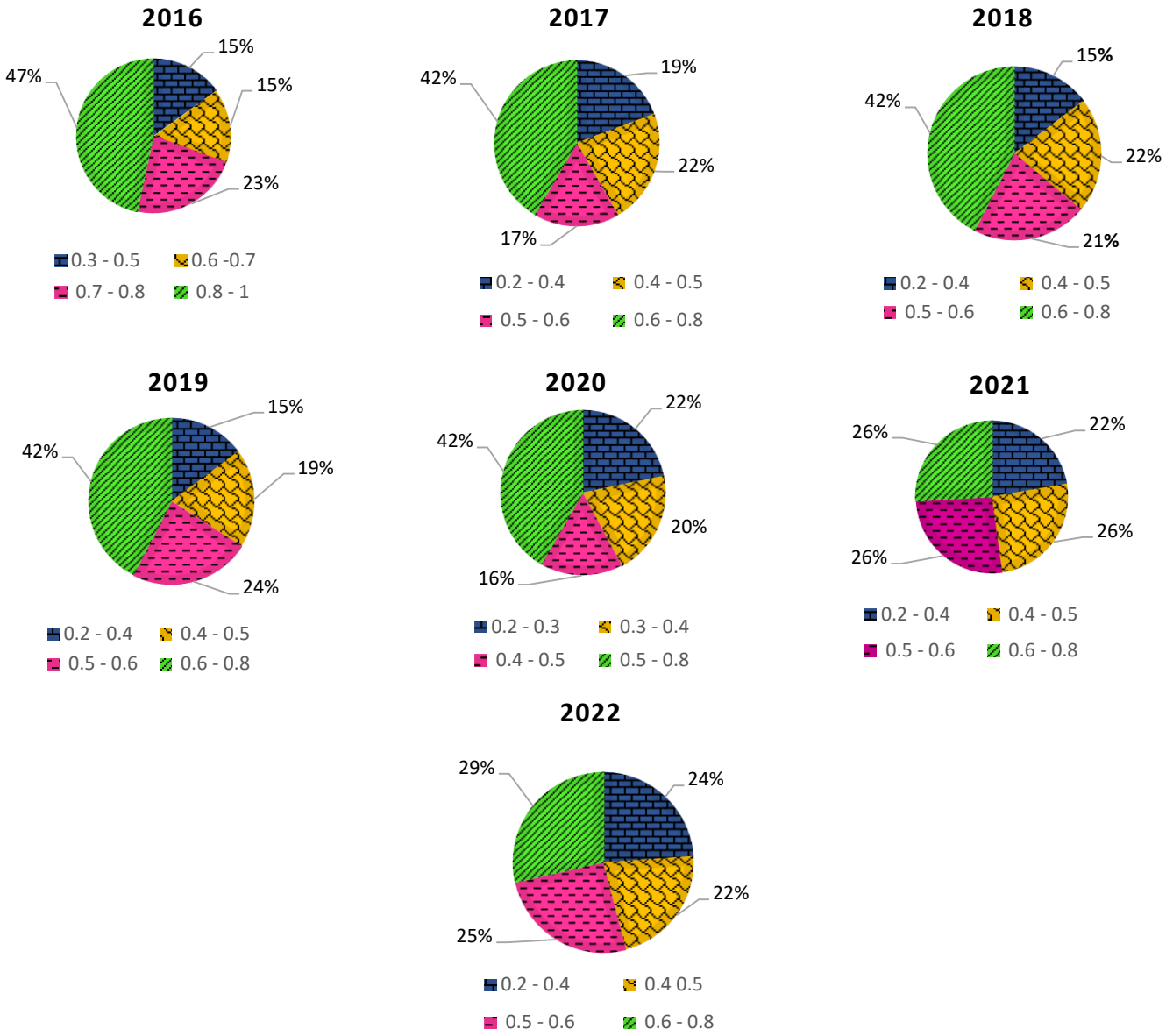

Fig. 13. Percentage of the VHI classes in Tajan watershed.

CONCLUSION

The study results showed that, when the amount of vegetation cover in the Tajan watershed was high, the LST in its various regions was low, but with decreasing vegetation cover, the LST increased in the watershed. Also, the results of the LST index in residential and barren areas of Tajan watershed indicated an increasing trend during the ten years, exhibiting the land use changes effect on LST. In other words, the trend of increasing temperature displays a direct relationship with the growth of these areas and a drop in the NDVI value. The transformation of the natural landscape including water, soil and plants (factors influencing the adjustment and reduction of the land surface temperature) into an artificial landscape including cement, asphalt, road, street, paving, chemicals and metals creates some changes in absorption, diffusion and its reflection of solar energy. Also, simultaneously the increase in urban areas causes an elevation in LST in these areas. The continuation of this trend will cause the phenomenon of heat islands and severe drought in Tajan watershed. Since this watershed has always faced big and small droughts, its geographical location and natural conditions are such that in the near future it will experience droughts of low and high density. Therefore, for decreasing the damage caused by drought, it is necessary to know the characteristics of drought. The results of the VCI, VHI, TCI, and SAVI drought index maps showed that the mentioned indices are increasing in Tajan watershed between 2013 and 2022. In future years, it will face the highest rate of drought, indicating a wide risk in the watershed. Because of the drying up of Tajan

watershed and the abandonment of agricultural lands and water sources shortage, especially underground water sources shortage or the lack of alternative surface water sources, the drought will increase. Therefore, the risk of drought threatens the agricultural, environmental, social, and economic ecosystems of the watershed. If appropriate methods are not used to deal with it, this region of Iran will face many problems. Hence, the need to use comprehensive methods of water management in all sectors, including storage, transmission, and distribution is very necessary. Also, monitoring the drought of the watershed using satellite images can represent the density and extent of drought in areas with a lack of meteorological data. Therefore, the effectiveness of drought indices based on satellite time series data helps to plan the reduction of drought risks. Finally, the process of vegetation destruction is expected in the future. By employing the correct management methods, sustainable water distribution, regional negotiations, principled agriculture and the creation of optimal hydrological conditions as well as complementary studies for spatial monitoring of drought through satellite images and the ground measurements lead to slight changes in the cover and decreasing the land surface temperature. Also, it is possible to create drought forecasting systems by examining vegetation and climatic parameters such as temperature and humidity to reduce the damage of this phenomenon in the future.

ACKNOWLEDGEMENTS

We extend special thanks to Sari Agricultural Sciences and Natural Resources Universities (SANRU), department of agricultural engineering that helped us to do the paper.

REFERENCES

Ashrafi, S, Kerachian, R, Pourmoghim, P, Behboudian, M & Motlaghzadeh, K 2022, Evaluating and improving the sustainability of ecosystem services in river basins under climate change. *Science of the Total Environment*, 3: 806, 150702, https://doi.org/10.1016/j.scitotenv.2021.150702.

Amirnejad, H, Hosseini, S & Azadi, H 2025, Evaluation and valuation of Tajan river basin ecosystem services. *Ecohydrology & Hydrobiology*, 25(1): 238-249, https://doi.org/10.1016/j.ecohyd.2024.03.005.

Bai, K, Liu, Ch, Shi, R & Gao, W 2012, Analysis of spatial-temporal characteristic of drought in Southwest China in 2010 by using MODIS-based Normalized Difference Drought Index. *Journal of Geo-Information Science*, 14(1): 32-40, https://doi.org/10.3724/SP.J.1047.2012.00032.

Bayarjargal, Y, Karnieli, A, Bayasgalan, M, Khudulmur, S, Gandush, C & Tucker, CJ 2006, A comparative study of NOAA–AVHRR derived drought indices using change vector analysis. *Remote Sensing of Environment*, 105(1): 9-22, https://doi.org/10.1016/j.rse.2006.06.003.

Chang, S, Chen, H, Wu, B, Nasanbat, E, Yan, N, Davdai B 2021, A practical satellite-derived vegetation drought index for arid and semi-arid grassland drought monitoring. *Remote Sensing*, 13: 414. https://doi.org/10.3390/rs13030414.

Comber, A & Wulder, M 2019, Considering spatiotemporal processes in big data analysis: Insights from remote sensing of land cover and land use. *Trans GIS*, 23(5): 879-891, https://doi.org/10.1111/tgis.12559.

Du, TLT, Bui, D, Nguyen, MD & Lee, H 2018, Satellite-based, multi-indices for evaluation of agricultural droughts in a highly dynamic tropical catchment, Central Vietnam. *Water* (Switzerland), 10(5): 1-24. https://doi.org/10.3390/w10050659.

Elhag, KM & Zhang, WC 2018, Monitoring and assessment of drought focused on its impact on sorghum yield over Sudan by using meteorological drought indices for the period 2001–2011. *Remote Sensing*, 10(8): 1231, https://doi.org/10.3390/rs10081231.

Eze, E, Girma, A, Zenebe, A, Kourouma, JM & Zenebe, G 2020, Exploring the possibilities of remote yield estimation using crop water requirements for area yield index insurance in a datascarce dryland. *Journal of Arid Environments*, 183: 104-261, https://doi.org/10.1016/j.jaridenv.2020.104261.

Feng, Y, Gao, C, Tong, X, Chen, S, Lei Z & Wang, J 2019, Spatial patterns of land surface temperature and their influencing factors: A case study in Suzhou, China. *Remote Sensing*, 11(2): 182-194, https://doi.org/10.3390/rs11020182.

Gidey, E, Dikinya, O, Sebego, R, Segosebe, E & Zenebe, A 2018, Analysis of the long – term agricultural drought onset, cessation, duration, frequency, severity and spatial extent using Vegetation Health Index (VHI) in Raya and its environs, Northern Ethiopia. Northern Ethiopia. *Environmental Systems Research*, 7(1): 13-29, https://doi.org/10.1186/s40068-018-0115-z.

Guha, S, Govil, H, & Besoya, M 2020, An Investigation on Seasonal Variability between LST and NDWI in an urban environment using Landsat satellite data. Geomat. *Natural Hazards and Risk*, 11: 1319-1345, https://doi.org/10.1080/19475705.2020.1789762.

Guo, H, Bao, A, Liu, T, Ndayisaba, F, He, D, Kurban, A & Maeyer PD 2017, Meteorological drought analysis in the Lower Mekong Basin using satellite-based long-term CHIRPS product. *Sustainability*, 9 (6): 901, https://doi.org/10.3390/su9060901.

Harishnaika, N, Ahmed, SA, Kumar, S, Arpitha, M 2022, Computation of the spatio-temporal extent of rainfall and long-term meteorological drought assessment using standardized precipitation index over Kolar and Chikkaballapura districts, Karnataka during, 1951–2019. *Remote Sensing Applications: Society and Environment*, 27:100768. https://doi.org/10.1016/j.rsase.2022.100768.

Hosseini, S, Oladi, J, Amirnejad, H 2021a, The evaluation of environmental, economic and social services of national parks. *Environment, Development and Sustainability*, 23: 9052-9075. https://doi.org/10.1007/ s10668-020-01011-6. [In Persian].

Huang, S, Tang, L, Hupy, JP, Wang, Y & Shao G 2021, A commentary review on the use of normalized difference vegetation index (NDVI) in the era of popular remote sensing. *Journal of Forestry Research*, 32(6): 1-6, http://dx.doi.org/10.1007/s11676-020-01176-w.

Ibrahim, M & Abu-Mallouh, H 2018, Estimate land surface temperature in relation to land use types and geological formations using spectral remote sensing data in northeast Jordan. *Open Journal of Geology*, 8(02): 174-185. http://dx.doi.org/10.4236/ojg.2018.82011.

Jahanifar, K, Amirnejad, H, Abedi, Z, Vafaeenejad, A 2017, Economic and environmental feasibility of rangeland conversion to other land uses in East of Mazandaran province. *Journal of Rangeland*, 11(2): 207-221, [In Persian].

Jiao, W, Zhang, L, Chang, Q, Fu, D, Cen, Y & Tong, Q 2016. Evaluating an Enhanced Vegetation Condition Index (VCI) Based on VIUPD for Drought Monitoring in the Continental United States. *Remote Sensing*, 8(3): 224-245, https://doi.org/10.3390/rs8030224.

Kapuka, A, Dobor, L, & Hlásny, T 2022, Climate change threatens the distribution of major woody species and ecosystem services provision in Southern Africa. *Science of the Total Environment*, 850: 158006. https://doi.org/10.1016/j.scitotenv.2022.158006.

Karnieli, A, Bayasgalan, M, Bayarjargal, Y, Agam, N, Khudulmur, S & Tucker, CJ 2006, Comments on the use of the vegetation health index over Mongolia. *International Journal of Remote Sensing*, 27(10): 2017-2024, https://doi.org/10.1080/01431160500121727.

Karnieli, A, Ohana-Levi, N, Silver M, Paz-Kagan, T, Panov N, Varghese, D, Chrysoulakis, N & Provenzale, A 2019a, Spatial and seasonal patterns in vegetation growth-limiting factors over Europe. *Remote Sensing*, 11: 2406. https://doi.org/10.3390/rs11202406.

Kayet, N, Pathak, K, Chakrabarty, A & Sahoo, S 2016, Spatial impact of land use/land cover change on surface temperature distribution in Saranda Forest, Jharkhand. *Modelling Earth Systems and Environment*, 2(3): 127-139, https://link.springer.com/article/10.1007/s40808-016-0159-x.

Ketelsen, T, Sawdon, J & Rasaenen, T 2020, Monitoring the quantity of water flowing through the Upper Mekong Basin under natural (unimpeded) conditions- Rapid Review, https://www.amperes.com.au/s/AMPERES-Review_Basist-et-al_ Lancang-flows-19-April-2020.pdf.

Khalil, AA, Hassanein MM, Ouldbdey B, Katlan B & Essa, Y 2013, Drought monitoring over Egypt by using MODIS land surface temperature and normalized difference agro-droughts in Southwest of China using MODIS satellite data. *Journal of Integrative Agriculture*. 12(1): 159-168, http://www.sciencepub.net.

Kloos, S, Yuan, Y, Castelli, M & Menzel, A 2021, Agricultural Drought Detection with MODIS Based Vegetation Health Indices in Southeast Germany. *Remote Sensing*, 13: 3907, https://doi.org/10.3390/ rs13193907.

Kogan, FN 1995, Application of vegetation index and brightness temperature for drought detection. *Advances in Space Research*, 15(11): 91-100, https://doi.org/10.1016/0273-1177 (95)00079-T.

Kong, D, Zhang, Y, Xihui, G & Wang, D 2019. A robust method for reconstructing global MODIS EVI time series on the Google Earth Engine. ISPRS J. Photogram. *Remote Sensing*, 155: 13-24, https://doi.org/10.1016/j. isprsjprs.2019.06.014.

Kumari, N, Srivastava, A & Dumka, UC 2021, A Long-Term Spatiotemporal Analysis of Vegetation Greenness over the Himalayan Region Using Google Earth Engine. *Climate*, 9: 109. http://dx.doi.org/

10.3390/cli9070109.

Lei, Q, Zhang, X, Wang, X, He, X & Shang, C 2019, Responses of vegetation index to meteorological drought in Dongting Lake Basin based on MODIS-EVI and CI. *Resources and Environment in the Yangtze Basin*, 28: 981-993.

Liang, L, Sun, Q, Luo, X, Wang, J, Zhang, L, Deng, M, Di, L & Liu, Z 2017, Long-term spatial and temporal variations of vegetative drought based on vegetation condition index in China. *Ecosphere*, 8: 1-15. http://dx.doi.org/10.1002/ecs2.1919.

Ma, Sh, Wang, L, Jiang, J, Chu L & Zhang, J 2021, Threshold effect of ecosystem services in response to climate change and vegetation coverage change in the Qinghai-Tibet Plateau ecological shelter. *Journal of Cleaner Production*. 318: 128592, https://doi.org/10.1016/j.jclepro.2021.128592.

Markham, BL & Barker, JL 1985, Spectral characterization of the Landsat Thematic Mapper sensors. *International Journal of Remote Sensing*, 6(5): 697-716. https://doi.org/10.1080/01431168508948492.

Masitoh, F & Rusydi AN 2019, Vegetation Health Index (VHI) analysis during drought. *Earth and Environmental Science*. 389. 012033. doi:10.1088/1755-1315/389/1/012033.

Mishra, A, Singh, VP 2011, Drought modelling: A review. *Journal of Hydrology*, 403(2): 157–175. https://doi.org/10.1016/j.jhydrol.2011.03.049.

Mollmann, J, Buchholz, M & Musshoff, O 2019, Comparing the Hedging Effectiveness of Weather Derivatives Based on Remotely Sensed Vegetation Health Indices and Meteorological Indices. *Weather, Climate, and Society*, 11: 33–48. http://dx.doi.org/10.1175/WCAS-D-17-0127.1.

Morabito, M, Crisci, A, Messeri, A, Orlandini, S, Raschi, A, Maracchi, G & Munafo, M 2016, The impact of built up surfaces on land surface temperatures in Italian urban areas. *Science of the Total Environment*, 551-552(5): 317-326. http://dx.doi.org/10.1016/j.scitotenv.2016.02.029.

Mulugeta, S, Fedler, C, Ayana, M & Ayana, M 2019, Analysis of long-term trends of annual and seasonal rainfall in the Awash River Baser Ethiopia. *Water*, 11(7): 1498, http://dx.doi.org/10.3390/w11071498.

Pei, F, Wu, Ch, Liu, X, Li, X, Yang, K, Zhou, Y, Wang, K, Xu, L & Xia, G 2018, Monitoring the vegetation activity in China using vegetation health indices. *Agricultural and Forest Meteorology*, 248: 215-227. https://doi.org/10.1016/j.agrformet.2017.10.001.

Pourhabib, Y, Fataei, E, Nasehi, F, Khanizadeh, B & Saadati, H 2025, Monitoring the spatial changes of river water quality through the fusion of Landsat 8 images and statistical models (A case study: Sefidroud River, Northwest Iran). *Caspian Journal of Environmental Sciences*, 23(2): 315-326.

Rhee, J, Im, J & Carbone, G, 2010, Monitoring agricultural drought for arid and humid regions using multi-sensor remote sensing data. *Remote Sensing of Environment*. 114: 2875-2887, http://dx.doi.org/ 10.1016/j.rse.2010.07.005.

Rongali, G, Keshari, AK, Gosain, AK & Khosa, R 2017, Land surface temperature estimation algorithms from Landsat 8 thermal infrared sensor data of Beas River Basin, Himachal Pradesh, India. Conference: International Conference on Modelling of Environmental and Water Resources System, pp. 129-202.

RWCM 2022, Regional Water Company of Mazandaran.www.mzrw.ir.

Sannigrahi, S, Zhang Q, Joshi, P.K, Sutton P, Keesstra, S, Roy, P.S. h, Pilla, F & Basu, B *et al* 2020, Examining effects of climate change and land use dynamic on biophysical and economic values of ecosystem services of a natural reserve region. *Journal of Cleaner Production*, 257: 120424. https://doi.org/10.1016/ j. jclepro.2020.120424.

Sarker, Md, Latifur, R, Janet, N, Mansor Siti, A, Ahmad, BB, Shahid, S, Chung, E-S, Reid, J-S & Siswanto, E 2020, An integrated method for identifying present status and risk of drought in Bangladesh. *Remote Sensing*, 12 (17): 2686, https://doi.org/10.3390/rs12172686.

Sekertekin, A & Bonafoni, S 2020, Land Surface Temperature Retrieval from Landsat 5, 7, and 8 over Rural Areas: Assessment of Different Retrieval Algorithms and Emissivity Models and Toolbox Implementation. *Remote Sensing*, 12(2): 294, https://doi.org/10.3390/rs12020294

Shi, Y, Katzschner, L & Ng, E 2017, Modelling the fine-scale spatiotemporal pattern of urban heat island effect using land use regression approach in a megacity, *Science of the Total Environment*, 618(15): 891-904, https://doi.org/10.1016/j.scitotenv.2017.08.252.

Sobrino, JA, Jimenez- Munoz, JC & Paolinib, L 2004, Land surface temperature retrieval from Landsat TM. *Remote Sensing of Environment*, 90 (4): 434-440, http://dx.doi.org/10.1016/j.rse.2004.02.003.

Somvanshi, Sh & Kumari, M 2021, Comparative analysis of different vegetation indices with respect to atmospheric particulate pollution using sentinel data. *Applied*. 7: 100032. http://dx.doi.org/10.1016/j.acags.2020.100032.

Thiriot, A 1978, Zooplankton communities in the West African upwelling area. In: R. Boje, M. Tomzak (Eds.), Upwelling Ecosystems, Springer, Berlin, 32-61.

UNESCO, UN-Water 2020, United Nations world water development report 2020: Water and climate change. UNESCO, Paris.

Uniyal, B, Kosatica, E & Koellner, Th 2023, Spatial and temporal variability of climate change impacts on ecosystem services in small agricultural catchments using the Soil and Water Assessment Tool (SWAT). *Science of the Total Environment*, 875: 162520. https://doi.org/10.1016/j.scitotenv.2023.162520.

Wang, F, Wang, Z, Yang, H, Zhao, Y, Li, Z & Wu, J 2018, Capability of remotely sensed drought indices for representing the spatio–temporal variations of the meteorological droughts in the Yellow River Basin. *Remote Sensing*, 10 (11), 1834. https://doi.org/10.3390/rs10111834.

Wang, R, Cai, M, Ren, Ch, Bechtel, B, Xu, Y & Ng, E 2019, Detecting multi-temporal land cover change and land surface temperature in Pearl River Delta by adopting local climate zone, *Urban Climate*, 28: 1-16. http://dx.doi.org/10.1016/j.uclim.2019.100455.

Xiao, F, Li, Y-Z, Yun, D, Feng, L, Yi, Y, Qi, F & Xuan, B 2014. Monitoring perennial sub-surface waterlogged croplands based on MODIS in Jianghan Plain, middle reaches of the Yangtze River. *Journal of Integrative Agriculture*, 13(8): 1791-1801, https://doi.org/10.1016/S2095-3119 (13) 60563-8.

Xie, F & Fan, H 2021, Deriving drought indices from MODIS vegetation indices (NDVI/EVI) and Land Surface Temperature (LST): Is data reconstruction necessary? *The International Journal of Applied Earth* Observation *and Geoinformation*, 101; 102352. https://doi.org/10.1016/j.jag.2021.102352.

Xu, Y, Xie, Y, Wu X, Xie, Y, Zhang, T, Zou, Z, Zhang, R & Zhang, Z 2023, Evaluating temporal-spatial variations of wetland ecosystem service value in China during 1990–2020 from the donor side. *Journal of Cleaner Production*, 21: 137485. https://doi.org/10.1016/j.jclepro.2023.137485.

Zaharaddeen, I, Baba, II & Zachariah, A 2016, Estimation of land surface temperature of Kaduna metropolis, Nigeria using Landsat images. *Scientific World Journal*, 11(3): 36-42, https://doi.org/10.4236/ epe.2018.1010028.

Zambrano, F, Saavedra, M.L, Verbist, K & Lagos, O 2016, Sixteen years of agricultural drought Assessment of the Bio Region in Chile using a 250 m Resolution Vegetation Condition Index (VCI). *Remote Sensing*, 8(6):530. http://dx.doi.org/10.3390/rs8060530.

Zarandian, A, Yavari, A, Jafari, H & Amirnejad, H 2016, Modelling land use change impacts on water-related ecosystem services using a policy support system. *Environmental Sciences*, 13(4): 97-112.

Zhang, F, Kung, H, Johnson, V.C, LaGrone, B.I, & Wang, J 2018, Change detection of land surface temperature (LST) and some related parameters using Landsat image: a case study of the Ebinur Lake watershed, Xinjiang, China, *Wetlands*, 38(1): 65-80, http://dx.doi.org/10.1007/s13157-017-0957-6.

Zhang, L, Yao, Y, Bei, X, Jia, K, Zhang, X & Xie, X *et al.* 2019, Assessing the remotely sensed evaporative drought index for drought monitoring over Northeast China. *Remote Sensing*, 11(17). https://doi.org/10.3390/rs11171960.

Zhen, Z, Chen, S, Yin, T, Chavanon, E, Lauret, N, Guilleux, J, Henke, M, Qin, W, Cao, L, Li, J, Lu, P & Gastellu-Etchegorry, JP 2021, Using the negative soil adjustment factor of Soil Adjusted Vegetation Index (SAVI) to resist saturation effects and estimate Leaf Area Index (LAI) in dense vegetation areas. *Sensors*, 21: 2115, https://doi.org/10.3390/s21062115.

Zuhro, A, Tambunan, MP & Marko, K 2020, Application of vegetation health index (VHI) to identify distribution of agricultural drought in Indramayu Regency, West Java Province. *Environmental Earth Sciences*, 500: 12047, http://dx.doi.org/10.1088/1755-1315/500/1/012047.